

ARTICLE

# Neuronal interleukin-1 receptors mediate pain in chronic inflammatory diseases

Benoit Mailhot<sup>1</sup>, Marine Christin<sup>2</sup>, Nicolas Tessandier<sup>3</sup>, Chaudy Sotoudeh<sup>4</sup>, Floriane Bretheau<sup>1</sup>, Roxanne Turmel<sup>1</sup>, Ève Pellerin<sup>1</sup>, Feng Wang<sup>5</sup>, Cyril Bories<sup>5</sup>, Charles Joly-Beauparlant<sup>6</sup>, Yves De Koninck<sup>5</sup>, Arnaud Droit<sup>6</sup>, Francesca Cicchetti<sup>7</sup>, Grégory Scherrer<sup>8,9</sup>, Eric Boilard<sup>3</sup>, Reza Sharif-Naeini<sup>2</sup>, and Steve Lacroix<sup>1</sup>

**Chronic pain is a major comorbidity of chronic inflammatory diseases. Here, we report that the cytokine IL-1 $\beta$ , which is abundantly produced during multiple sclerosis (MS), arthritis (RA), and osteoarthritis (OA) both in humans and in animal models, drives pain associated with these diseases. We found that the type 1 IL-1 receptor (IL-1R1) is highly expressed in the mouse and human by a subpopulation of TRPV1<sup>+</sup> dorsal root ganglion neurons specialized in detecting painful stimuli, termed nociceptors. Strikingly, deletion of the *Il1r1* gene specifically in TRPV1<sup>+</sup> nociceptors prevented the development of mechanical allodynia without affecting clinical signs and disease progression in mice with experimental autoimmune encephalomyelitis and K/BxN serum transfer-induced RA. Conditional restoration of IL-1R1 expression in nociceptors of IL-1R1-knockout mice induced pain behavior but did not affect joint damage in monosodium iodoacetate-induced OA. Collectively, these data reveal that neuronal IL-1R1 signaling mediates pain, uncovering the potential benefit of anti-IL-1 therapies for pain management in patients with chronic inflammatory diseases.**

## Introduction

Chronic pain is estimated to affect 20% of adults worldwide and correspondingly incurs a significant socioeconomic burden (Goldberg and McGee, 2011). Because patients suffering from chronic inflammatory diseases such as multiple sclerosis (MS), rheumatoid arthritis (RA), and osteoarthritis (OA) are more predisposed to pain than others, with ratios reaching 50% (Mifflin and Kerr, 2017), it is critical to understand the link between these diseases and chronic pain.

Chronic inflammatory diseases are characterized by dysfunctions with the immune system, resulting in elevated levels of proinflammatory mediators. Recent studies involving animal models of these diseases and human patients have suggested that the cytokine IL-1 $\beta$  contributes to inflammation in MS, RA, and OA (Cohen et al., 2004; Jenei-Lanzl et al., 2019; Lévesque et al., 2016; Mertens and Singh, 2009; Wojdasiewicz et al., 2014). The cellular signaling of IL-1 $\beta$  is known to occur via the type 1 IL-1 receptor (IL-1R1). Outside of the nervous system, IL-1R1 is

expressed at the cell surface of leukocytes and their precursors (Pietras et al., 2016). In the nervous system, expression of the IL-1R1 protein is thought to be mainly restricted to endothelial cells, both in normal and inflammatory conditions (Aubé et al., 2014; Lévesque et al., 2016; Li et al., 2011). Additionally, IL-1 $\beta$  can directly stimulate glial cells and neurons (Balasingam et al., 1994; Binshtok et al., 2008; Bruttger et al., 2015; Huang et al., 2011; Kawasaki et al., 2008; Liu et al., 2006; Smith et al., 2009; Takeda et al., 2007; Watkins and Maier, 2002; Yan and Weng, 2013). However, there are still striking inconsistencies in the literature regarding the expression of IL-1R1 and other inflammatory cytokine receptors on neurons in the nervous system (Cook et al., 2018). Furthermore, there are a number of incongruences regarding the inflammatory versus the neurophysiological effects of IL-1 $\beta$  (for reviews, see Allan et al., 2005; Liu and Quan, 2018).

Although chronic pain in these diseases was initially believed to be a consequence of inflammatory reactions, it was recently

<sup>1</sup>Axe Neurosciences du Centre de recherche du CHU de Québec-Université Laval et Département de médecine moléculaire de l'Université Laval, Québec, Canada; <sup>2</sup>Department of Physiology and Cell Information Systems Group, McGill University, Montreal, Canada; <sup>3</sup>Axe Maladies infectieuses et immunitaires du Centre de recherche du CHU de Québec-Université Laval et Département de microbiologie-infectiologie et d'immunologie de l'Université Laval, Québec, Canada; <sup>4</sup>Department of Anesthesiology, Perioperative and Pain Medicine, Stanford University, Palo Alto, CA; <sup>5</sup>Centre de recherche CERVO, Québec, Canada; <sup>6</sup>Axe Endocrinologie-néphrologie du Centre de recherche du CHU de Québec-Université Laval et Département de médecine moléculaire de l'Université Laval, Québec, Canada; <sup>7</sup>Axe Neurosciences du Centre de recherche du CHU de Québec-Université Laval et Département de psychiatrie et de neurosciences de l'Université Laval, Québec, Canada; <sup>8</sup>Department of Cell Biology and Physiology, University of North Carolina Neuroscience Center, The University of North Carolina at Chapel Hill, Chapel Hill, NC; <sup>9</sup>New York Stem Cell Foundation - Robertson Investigator, The University of North Carolina at Chapel Hill, Chapel Hill, NC.

Correspondence to Steve Lacroix: [Steve.Lacroix@crchul.ulaval.ca](mailto:Steve.Lacroix@crchul.ulaval.ca).

© 2020 Mailhot et al. This article is distributed under the terms of an Attribution-Noncommercial-Share Alike-No Mirror Sites license for the first six months after the publication date (see <http://www.rupress.org/terms/>). After six months it is available under a Creative Commons License (Attribution-Noncommercial-Share Alike 4.0 International license, as described at <https://creativecommons.org/licenses/by-nc-sa/4.0/>).

proposed that an intricate relationship between central nervous system (CNS) blood vessels and activated nociceptors, located in lumbar dorsal root ganglia (DRGs; Arima et al., 2012), could open a gateway to the accumulation of immune cells in the CNS (Arima et al., 2015). The neural pathway leading to the exacerbation of immune pathology was suggested to involve sensory neurons expressing transient receptor potential vanilloid 1 (TRPV1), but the mediators linking inflammation to pain remain elusive.

In MS, sustained pain can be attributable to multiple factors, including inflammation and ongoing CNS-related neuronal damage. However, in RA and OA, the affected tissue (cartilage) is aneural and avascular, which implies a more prominent role of inflammation in pain, as the surrounding innervated tissues of the articulations (e.g., muscles and bones) also need to be impacted (Sofat et al., 2011; Walsh and McWilliams, 2014). Supporting this is the fact that allodynia develops concomitantly with joint swelling in RA models. However, allodynia can persist after the resolution of inflammation, suggesting a persistent sensitization of nociceptive neurons (Christianson et al., 2010). Interestingly, it is believed that the key molecular mediators of pain in the DRGs and joints of RA and OA patients also involve TRPV1<sup>+</sup> nociceptors (Borbély et al., 2015; Kelly et al., 2015; Koda et al., 2016). As the lumbar DRGs innervating the articulations and the ones previously reported to influence experimental autoimmune encephalomyelitis (EAE) development show similarities, the molecular mechanisms involved in allodynia could be common across these inflammatory diseases.

In this study, we investigated the molecular mechanisms that underlie pain associated with IL-1 $\beta$ -dependent chronic inflammatory diseases such as EAE, RA, and OA. We demonstrate that macrophage- and neutrophil-derived IL-1 $\beta$  is found in close association with IL-1R1<sup>+</sup> sensory innervations and that IL-1 $\beta$  signaling is critical to the development of pain in these diseases.

## Results

### Mouse spinal dorsal roots are infiltrated by IL-1 $\beta$ -producing myeloid cells during EAE

Our group previously demonstrated the importance of myeloid cell-derived IL-1 $\beta$  in the initiation of neuroinflammation and the development of EAE (Lévesque et al., 2016; Paré et al., 2018). However, the proinflammatory paracrine actions of these cells in autoimmune inflammatory diseases remain elusive. Using transgenic mice expressing *Discosoma* red fluorescent protein (DsRed) under the control of the *Il1b* promoter, *pIl1b-DsRed* reporter mice, we aimed to track down the early invasion of IL-1 $\beta$ -producing cells in the CNS of mice with EAE. In early EAE stages (day of disease onset), we observed DsRed<sup>+</sup> cells in the lumbar dorsal roots, where sensory afferents that relay feedback from hind limbs are located (Fig. 1, A, B, and F). IL-1 $\beta$ -producing cells that accumulated in spinal dorsal roots were surrounded by axons immunostained for IL-1R1 (Fig. 1 C). Immunofluorescence confocal microscopy further revealed that cells producing pro-IL-1 $\beta$  colocalized with the myeloid cell marker CD11b (Fig. 1, D and E). As CD11b<sup>+</sup> myeloid cells comprise two major immune cell populations, namely monocytes/macrophages and neutrophils,

we next investigated whether one of these would be enriched in the infiltrates. IL-1 $\beta$ -producing (DsRed<sup>+</sup>) myeloid cells were identified as macrophages and neutrophils based on their expression of Iba1 and Ly6G, respectively (Fig. 1, F–J). Of interest is the fact that the infiltration of spinal nerve roots by IL-1 $\beta$ <sup>+</sup> myeloid cells preceded the appearance of paralysis, suggesting that this region may contribute to the clinical symptoms that develop early during the disease. These observations also suggest that the IL-1 $\beta$  produced by these cells could act directly on neurons.

### Articular nociceptors in the arthritic mouse hind limb are surrounded by IL-1 $\beta$ -producing myeloid cells

As for EAE, IL-1 $\beta$  signaling was shown to be critical to the pathogenesis of RA in mice (Ji et al., 2002; Nigrovic et al., 2007). Thus, we sought to determine whether IL-1 $\beta$  production could occur nearby the terminals of nociceptors that innervate the articular tissue in arthritic mice. To do so, we subjected *pIl1b-DsRed* reporter mice to the K/BxN serum-transfer arthritis model and assessed which cell types are responsible for the production of IL-1 $\beta$  in the inflamed ankle joint during the progression phase of RA using immunofluorescence microscopy. The analysis revealed the presence of several DsRed-expressing cells in the synovial and connective tissue layers of the diseased articular capsule (Fig. 2, A and E). Notably, these regions are innervated by sensory axons expressing the transient receptor potential cation channel subfamily V member 1 (TRPV1), an ion channel involved in the transmission of inflammatory pain (Fig. 2 B). Nociceptive TRPV1<sup>+</sup> axons coexpressed IL-1R1 and were closely associated with infiltrated IL-1 $\beta$ <sup>+</sup> cells (Fig. 2, A–D). Colocalization studies revealed that the majority of IL-1 $\beta$ <sup>+</sup> cells in the arthritic ankle joint coexpressed the neutrophil marker Ly6G, whereas the others were Iba1<sup>+</sup>, indicative of macrophages (Fig. 2, E–I). These results suggest that neutrophil- and macrophage-derived IL-1 $\beta$  not only play a key role in the initiation of inflammation during RA but also may trigger neuronal responses from specialized nociceptors.

### IL-1R1 expression defines a subtype of DRG nociceptors

To examine the subtype of sensory neurons that would respond to the release of IL-1 $\beta$ , we examined which subtypes express IL-1R1 by performing an immunohistochemical characterization of DRG sensory neurons. First, we observed that IL-1R1<sup>+</sup> DRG neurons have small-diameter cell bodies ( $12.45 \pm 1.35 \mu\text{m}$ ) and project to superficial laminae I and II of the spinal cord dorsal horn, indicating a role in pain transmission (Fig. 3, A–E). We thus evaluated the coexpression of IL-1R1 with markers that distinguish nociceptors from other types of sensory neurons, such as TRPV1, somatostatin (Sst), purinergic receptor P2X ligand-gated ion channel 3 (P2X3), calcitonin gene-related peptide (CGRP), isolectin B4 (IB4), and tyrosine hydroxylase (TH; Usoskin et al., 2015). We found that neurons expressing IL-1R1 represent ~10% of the entire DRG neuronal population (Fig. 3, F–M and N) and were all found to colocalize with TRPV1 (Fig. 3, F–M and O), a marker of peptidergic nociceptors in mice. This suggests that IL-1R1<sup>+</sup> neurons could play an important role in the perception of acute heat and/or inflammatory pain (Walder et al., 2012). Furthermore, all IL-1R1<sup>+</sup> DRG sensory

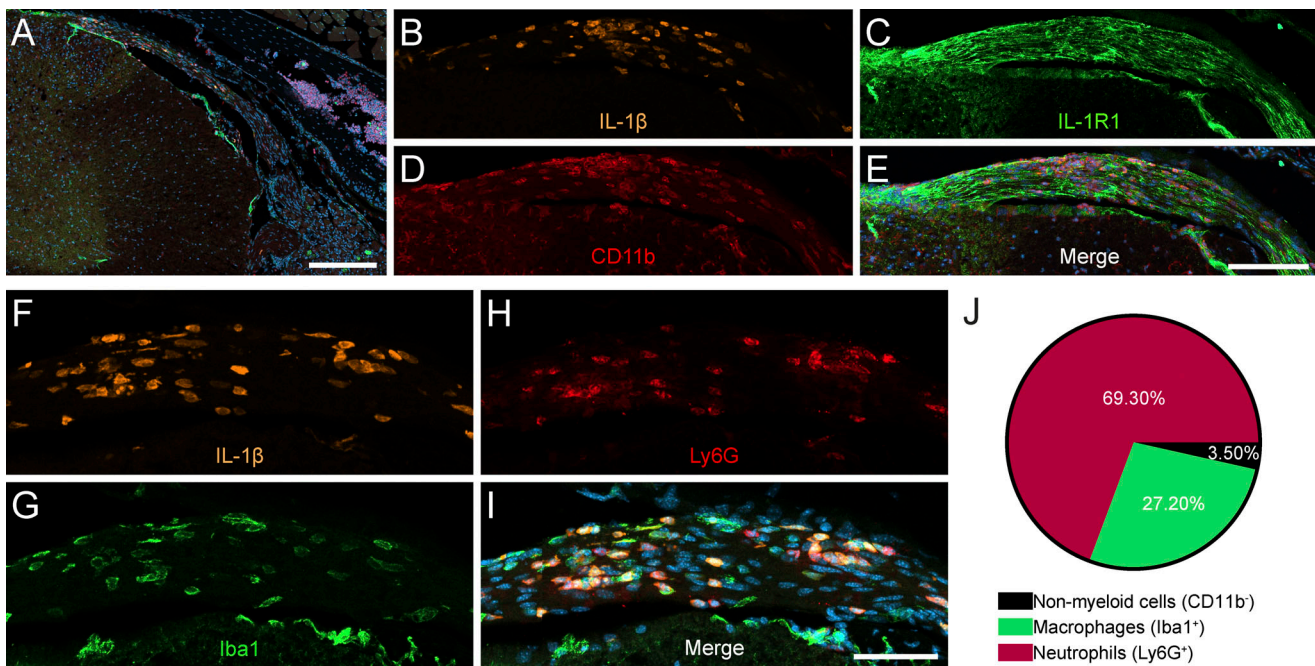


**Figure 1. IL-1 $\beta$ -producing myeloid cells are located nearby IL-1R1-expressing sensory neurons and their projections during EAE.** EAE was induced in *pIL1b-DsRed* mice, and immunofluorescence confocal microscopy imaging was performed to visualize the expression of IL-1 $\beta$  during the early phase (onset) of EAE. **(A)** IL-1 $\beta$  expression was detected in the dorsal root of spinal nerves projecting to the spinal cord. **(B–E)** Representative images showing the infiltration of CD11b-positive (+) myeloid cells (red cells in D) producing IL-1 $\beta$  (orange cells in B) in close proximity to IL-1R1<sup>+</sup> sensory axons (green in C) in the spinal dorsal root. **(F–I)** IL-1 $\beta$  (orange in F) is expressed by Ly6G<sup>+</sup> neutrophils (red in H) and Iba1<sup>+</sup> macrophages (green in G) that infiltrated the spinal dorsal root at EAE onset. Nuclear staining (DAPI) is shown in blue (E and I) in the merged images. **(J)** Quantification of colocalization for DsRed (IL-1 $\beta$ ) and markers of neutrophils (Ly6G) and macrophages (Iba1;  $n = 4$  mice total). Data are presented as a percentage of all DsRed<sup>+</sup> cells out of 500 DsRed<sup>+</sup> cells. Scale bars: 200  $\mu$ m (A); 100  $\mu$ m (E); and 50  $\mu$ m (I).

neurons also colocalized with P2X3, a marker of nonpeptidergic (NP) nociceptors, suggesting that IL-1R1<sup>+</sup> neurons might have mixed properties (Fig. 3 O). We also observed that ~25% of IL-1R1<sup>+</sup> DRG neurons coexpressed Sst, while 50% of Sst<sup>+</sup> neurons expressed IL-1R1 (Fig. 3, O and P). IL-1R1<sup>+</sup> DRG neurons did not bind IB4 (Fig. 3, F–I, O, and P) or express TH (Fig. 3, O and P), which indicates that IL-1R1 is absent from most NP C nociceptors

and is not expressed by C low-threshold mechanoreceptors. Interestingly, relatively few IL-1R1<sup>+</sup> neurons expressed CGRP protein ( $6.3\% \pm 8.4\%$ ; Fig. 3 O). These results identify IL-1R1 as a new marker that defines a population of nociceptors with mixed peptidergic/NP properties.

Adult mouse DRG neurons have been classified into different sensory subtypes based on their gene expression profiles

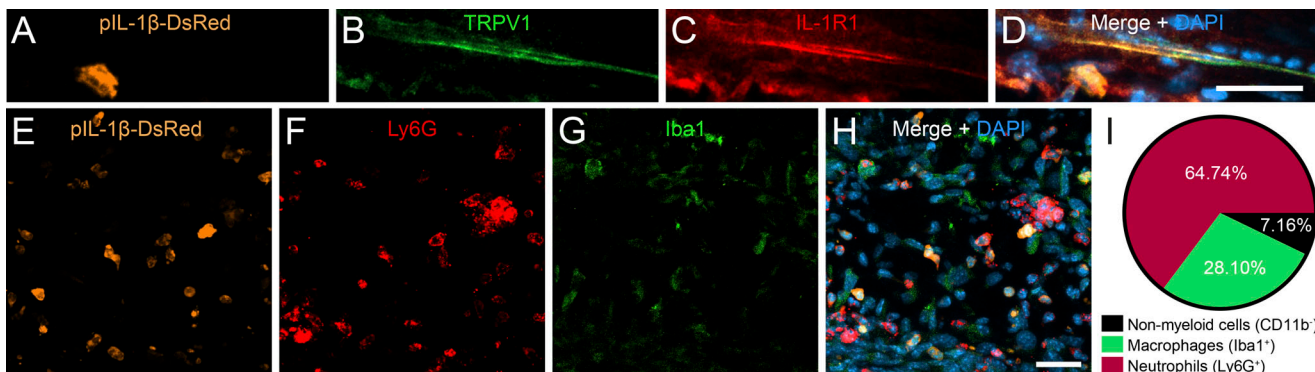


**Figure 2. IL-1 $\beta$  is produced in close association to IL-1R1<sup>+</sup> sensory innervation of the ankle joint in a mouse model of RA.** RA was induced in *pIL1b-DsRed* mice by K/BxN serum transfer, and immunofluorescence microscopy was performed to visualize the expression of IL-1 $\beta$  and its receptor, IL-1R1, during the early phase of disease. **(A–D)** IL-1 $\beta$ -expressing cells in the periarticular region of the inflamed ankle joint are located near IL-1R1<sup>+</sup> TRPV1<sup>+</sup> fibers 4 d after serum transfer. **(E–H)** Representative confocal images showing that IL-1 $\beta$  (orange pseudocolor in E) is mainly expressed by infiltrating Ly6G<sup>+</sup> neutrophils (red cells in F) and Iba1<sup>+</sup> macrophages (green in G). Nuclear staining (DAPI) is shown in blue (D and H) in the merged images. **(I)** Quantification of colocalization for DsRed (IL-1 $\beta$ ) and markers of neutrophils (Ly6G) and macrophages (Iba1). Data are presented as a percentage of all DsRed<sup>+</sup> cells ( $n = 3$  mice; a total of 500 DsRed<sup>+</sup> cells spread across all animals were counted). Scale bars: 20  $\mu$ m (D) and 25  $\mu$ m (H).

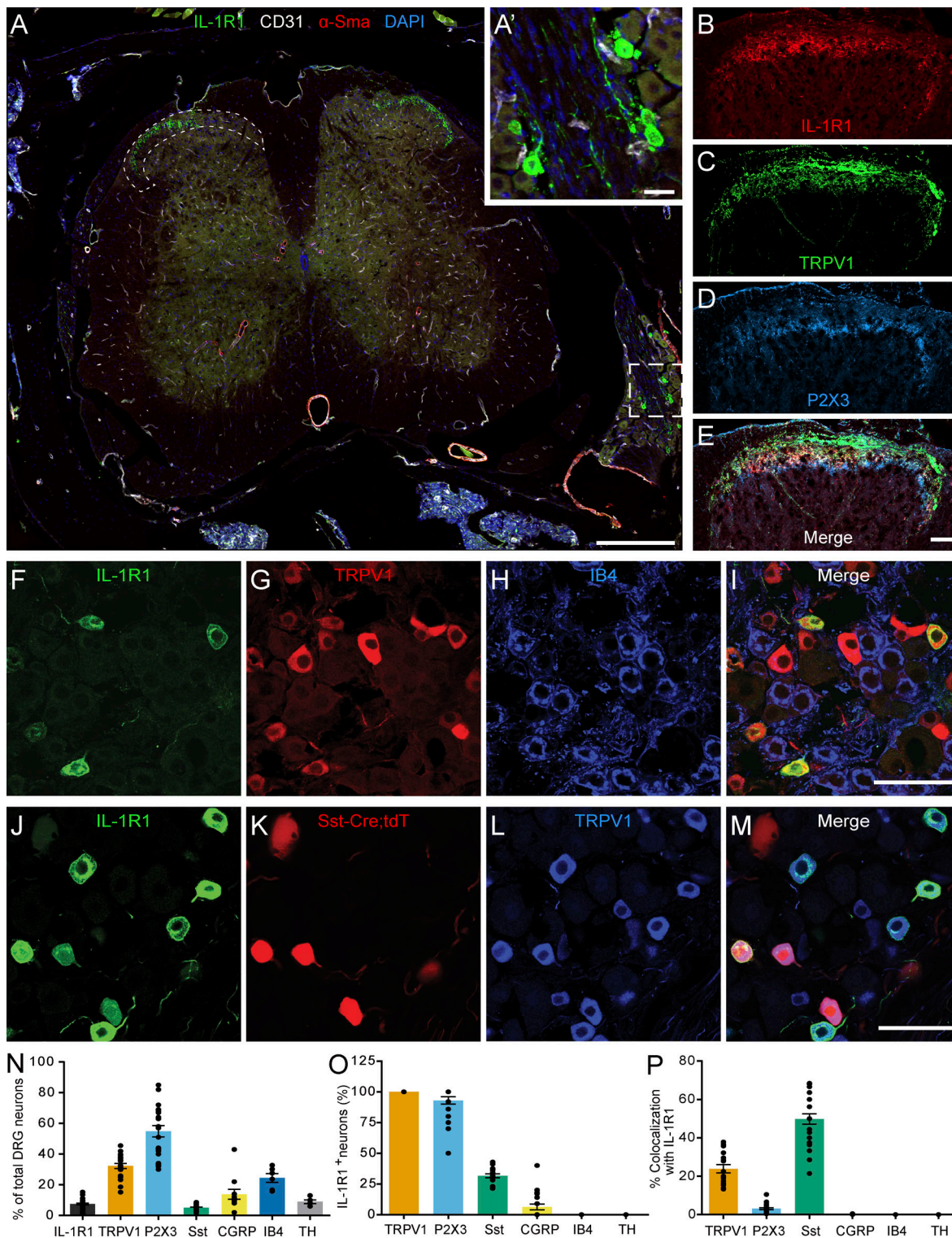


**Figure 3. IL-1R1 is expressed by TRPV1<sup>+</sup> DRG neurons in mice.** (A) Immunofluorescence confocal microscopy of spinal cord sections from C57BL/6 mice shows that IL-1R1 (green) is expressed by a subset of DRG neurons (inset A') that projects to laminae I and II of the dorsal horn (delineated by dotted lines). Antibodies directed against CD31 (white) and  $\alpha$ -smooth muscle actin ( $\alpha$ -SMA; red) were respectively used to stain blood vessel endothelial cells and pericytes/fibroblasts, while cell nuclei were counterstained with DAPI (blue). (B–E) Representative confocal images showing IL-1R1 (B), TRPV1 (C), and P2X3 (D) expression in the spinal cord dorsal horn. (F–I) DRG sections from naive C57BL/6 mice were immunostained with antibodies against IL-1R1 (F), TRPV1 (G), and IB4 (H) to characterize the subtypes of neurons expressing IL-1R1. (J–M) The colocalization of IL-1R1 was also assessed in *Sst<sup>Cre</sup>::Rosa26-tdTomato* mice, in which tandem dimer Tomato fluorescence (tdT) is driven by the *Sst* promoter. (N) Quantification of the percentage of DRG neurons expressing IL-1R1, TRPV1, P2X3, Sst, CGRP, IB4, and TH. (O) Quantification of the percentage of IL-1R1<sup>+</sup> DRG neurons coexpressing commonly used markers of sensory neuron subtypes. (P) Percentage of TRPV1<sup>+</sup>, P2X3<sup>+</sup>, Sst<sup>+</sup>, CGRP<sup>+</sup>, IB4<sup>+</sup>, and TH<sup>+</sup> neurons coexpressing IL-1R1 ( $n = 15$  mice). Data are shown as mean  $\pm$  SEM. Scale bars: 200  $\mu$ m (A); 25  $\mu$ m (A'); 50  $\mu$ m (E); 50  $\mu$ m (I); and 50  $\mu$ m (M).

(Usoskin et al., 2015; Zeisel et al., 2018). Having established that IL-1R1<sup>+</sup> DRG neurons are small-diameter TRPV1<sup>+</sup> P2X3<sup>+</sup> IB4<sup>neg</sup> CGRP<sup>neg</sup> C-fiber<sup>+</sup> (Fig. 3 and Fig. 4, A–F), we compared our immunofluorescence results with single-cell RNA sequencing (scRNA-seq) data from dissociated lumbar DRG neurons. This comparison indicated that IL-1R1<sup>+</sup> DRG neurons mainly correspond to a subset of the NP3/PSNP6 cluster of sensory neurons (Fig. 4, G and H). We next performed a detailed analysis of publicly available RNA-seq data from adult mouse DRG neurons to identify neurotransmitters and neuromodulators involved in the IL-1R1-mediated pain response, taking advantage of the open source database produced by the Linnarsson group (Usoskin et al., 2015; Zeisel et al., 2018). This analysis confirmed immunohistochemical findings showing that Sst, but not CGRP (encoded by the *Calca* gene), is strongly expressed in NP3/PSNP6 sensory neurons (Fig. 4 I and Table S1). Furthermore, the bioinformatic analysis led to the identification of several other genes coding for neurotransmitters and neuromodulators enriched in the NP3/PSNP6 subpopulation and which may be involved in the nociceptive effects of IL-1 $\beta$ , such as *Grpr*, *Cck*, *Nts*, *Scg2*, *Pthlh*, *Cysltr2*, *Nms*, *Nppb*, and *Mc3r*.

#### Human TRPV1<sup>+</sup> DRG sensory neurons express IL-1R1

We next investigated whether human DRGs also express IL-1R1. To this end, we immunolabeled human lumbar DRG sections with antibodies directed against IL-1R1, TRPV1, and CGRP. First, we confirmed the specificity of the anti-IL-1R1 antibody by performing IL-1R1 immunostaining in fresh frozen human DRG sections that had previously been incubated with a solution that contained either an excess of the IL-1 receptor antagonist anakinra, thus preventing subsequent binding of the primary antibody to the IL-1R1 antigen or no blocking agent (Fig. 5, A and B). As demonstrated, IL-1R1 immunoreactivity was not detected in DRG sections preincubated with anakinra. As observed in mice, we found that a subpopulation of neurons coexpressed IL-1R1 and TRPV1 in human DRGs (Fig. 5, C–N). The percentage of DRG neurons that expressed IL-1R1 was higher in humans than in mice, with a ratio of 20% compared with 10% in mice (Fig. 5 O). Another notable difference between humans and mice is that most IL-1R1<sup>+</sup> TRPV1<sup>+</sup> DRG sensory neurons also coexpressed CGRP (79.2%  $\pm$  10.0%; Fig. 5 P).

#### Activation of IL-1R1 in TRPV1<sup>+</sup> DRG sensory neurons triggers pain in chronic inflammatory diseases

To examine the functional role of IL-1R1 receptors expressed in nociceptors, we took advantage of transgenic mice constitutively lacking IL-1R1 (*Il1r1*<sup>-/-</sup> mice) and mice in which the *Il1r1* gene was deleted specifically in TRPV1<sup>+</sup> neurons (referred hereafter to as *Trpv1*<sup>Cre::Il1r1<sup>fl/fl</sup> mice) and evaluated the response to IL-1 $\beta$ . First, we confirmed the specificity of the *Trpv1*<sup>Cre::Il1r1<sup>fl/fl</sup> mouse line by showing the absence of IL-1R1 protein in DRG tissues (Fig. 6, A–D). Note that the specificity of the *Il1r1*<sup>-/-</sup> (*Il1r1*<sup>tr/r</sup>) mouse line has been extensively characterized elsewhere (Liu et al., 2019, 2015). Next, we injected recombinant murine (rm) IL-1 $\beta$  directly into the mouse sciatic nerve and assessed activation of this neuronal population. Here, expression of the transcription factors Fos and cyclic AMP response element-binding protein</sup></sup>

(CREB) was used as markers of cell activation (Lacroix et al., 1996; Segond von Banchet et al., 2016; Senger et al., 2019). Immunolabeling for Fos and phosphorylated CREB (pCREB) in tissue sections from WT mice treated with rmIL-1 $\beta$  confirmed that TRPV1<sup>+</sup> DRG neurons are activated as early as 4 h after injection (Fig. 6, E–P). Further analysis revealed that the marked up-regulation of Fos and pCREB proteins induced by the IL-1 $\beta$  treatment was prevented in *Trpv1*<sup>Cre::Il1r1<sup>fl/fl</sup> mice (Fig. 6 Q).</sup>

To determine whether IL-1 $\beta$  directly induces a neuronal response, we used video-rate two-photon microscopy to conduct in vivo calcium imaging in DRG neurons of IL-1 $\beta$ -treated *Trpv1*<sup>Cre</sup> knock-in mice transduced with Cre-dependent viruses expressing the calcium sensor GCaMP6s. No spontaneously occurring calcium response was detected in the GCaMP6s-transduced sensory neurons. Although no significant response was detected with vehicle application, we found that application of rmIL-1 $\beta$  to the exposed L4/L5 DRGs of mice induced a transient calcium response in a small subset of GCaMP6s-labeled sensory neurons (Fig. 6, R–V). These data suggest direct activation of TRPV1<sup>+</sup> sensory neurons by IL-1 $\beta$  under in vivo condition, consistent with a previously reported in vitro effect (Binshtok et al., 2008).

Since TRPV1<sup>+</sup> neurons play an important role in the perception of normal nociception (Bölskei et al., 2005), we next assessed whether deficiency in IL-1R1 affects mechanical and thermal behaviors under noninflammatory conditions. Importantly, constitutive knockout of the *Il1r1* gene did not impair mechanical (Fig. 6 W) or thermal (Fig. 6, X and Y) nociceptive responses. We then took advantage of the IL-1R1-restored mouse line (Liu et al., 2015), which exhibits an IL-1R1-knockout phenotype that can be reversed in a cell-specific manner by Cre-mediated recombination, to investigate whether IL-1R1<sup>+</sup> neurons play an important role in the perception of pain after inflammation. For this, we injected nociceptor-specific IL-1R1-restored mice, designated hereafter as *Trpv1*<sup>Cre::Il1r1<sup>tr/r</sup> mice, in the knee with rmIL-1 $\beta$  and monitored the allodynic response using the knee-bend test (Ferreira-Gomes et al., 2008; He et al., 2017). In both WT and *Trpv1*<sup>Cre::Il1r1<sup>tr/r</sup> mice, the injection of IL-1 $\beta$  in the knee capsule produced a transient allodynia during which gentle movements of the knee were associated with nocifensive behaviors. This period peaked between 4 and 24 h after injection. *Il1r1*<sup>-/-</sup> mice, however, did not show any allodynia after rmIL-1 $\beta$  injection (Fig. 6 Z). This result indicates that IL-1 $\beta$  can directly stimulate the TRPV1<sup>+</sup> DRG sensory neurons when released close to their IL-1R1-expressing axons.</sup></sup>

Mice subjected to active EAE, a common mouse model of MS, were previously found to develop pain-related behaviors such as mechanical allodynia, but not temperature hypersensitivity, before disease onset (Olechowski et al., 2009). Given that mice deficient for IL-1 $\beta$  or IL-1R1 are resistant to EAE (Fig. 7 A), we next investigated the importance of IL-1R1 in pain in an animal model in which the immune response underlying autoimmune encephalitis is intact. Since we previously established that 100% of IL-1R1<sup>+</sup> DRG neurons coexpress TRPV1 (Fig. 3 O) and that these nociceptors become unresponsive to IL-1 $\beta$  when the *Il1r1* gene is deleted (Fig. 6, A–Q), we tested *Trpv1*<sup>Cre::Il1r1<sup>fl/fl</sup> mice in the EAE model. We observed that EAE develops in a similar manner in terms of the time course and severity of motor</sup>

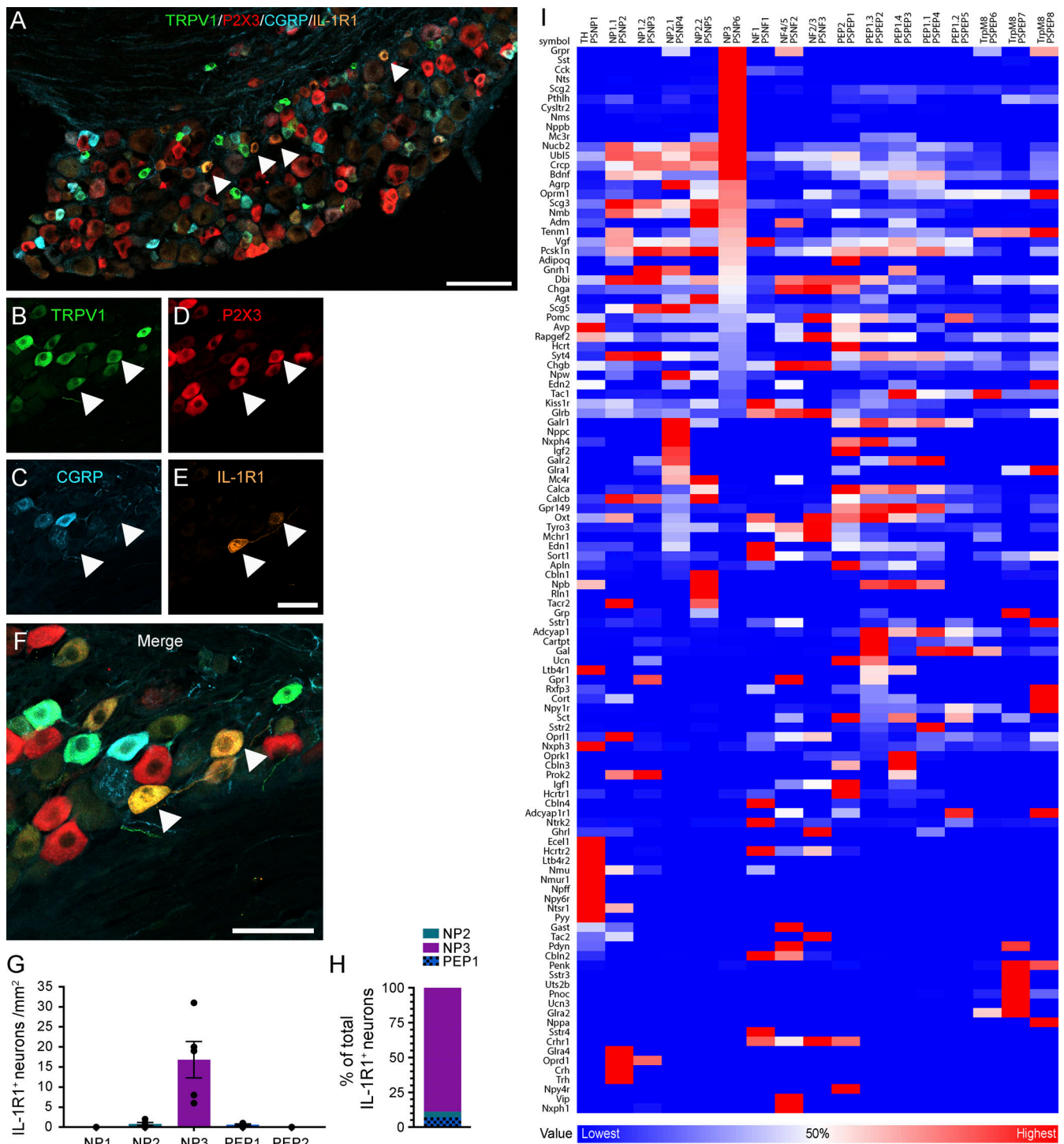


**Figure 4. IL-1R1 is expressed by a subset of NP nociceptive sensory neurons in mice. (A–F)** Representative confocal images showing immunostaining of DRG sections with antibodies against TRPV1 (green), P2X3 (red), CGRP (blue), and IL-1R1 (orange). The white arrowheads point to examples of TRPV1<sup>+</sup> P2X3<sup>+</sup> IL-1R1<sup>+</sup> neurons. **(G)** Quantification of the total number of IL-1R1-expressing neurons (per millimeter squared) in the L4–L6 DRGs, divided according to the sensory neuron classification proposed by [Uosokin et al. \(2015\)](#): NP1 (TRPV1<sup>−</sup> P2X3<sup>−</sup> CGRP<sup>−</sup>), NP2 (TRPV1<sup>+</sup> P2X3<sup>+</sup> CGRP<sup>+</sup>), NP3 (TRPV1<sup>+</sup> P2X3<sup>−</sup> CGRP<sup>−</sup>), PEP1 (TRPV1<sup>+</sup> P2X3<sup>−</sup> CGRP<sup>+</sup>), and PEP2 (TRPV1<sup>−</sup> P2X3<sup>−</sup> CGRP<sup>+</sup>); *n* = 5 mice. **(H)** The counts shown in G are expressed as a percentage ratio of the three subpopulations of sensory neurons expressing TRPV1 (*n* = 5 mice). Data are shown as mean ± SEM (G and H). **(I)** Bioinformatic analysis of genes associated with neuropeptides, neuromodulators, and neurotransmitters in the different DRG neuronal subtypes using scRNA-seq raw data from [Zeisel et al. \(2018\)](#). The neuronal classification proposed by [Uosokin et al. \(2015\)](#) is also reported on top of the heatmap. For each gene, the heatmap shows the neuronal subtype with the highest (red) and lowest (blue) expression. White corresponds to 50% of the maximal expression for each gene. Sequential sorting was performed to visualize genes expressed specifically by the NP3 (PSNP6) population of DRG neurons. Scale bars: 100 μm (A); 50 μm (E); and 50 μm (F).

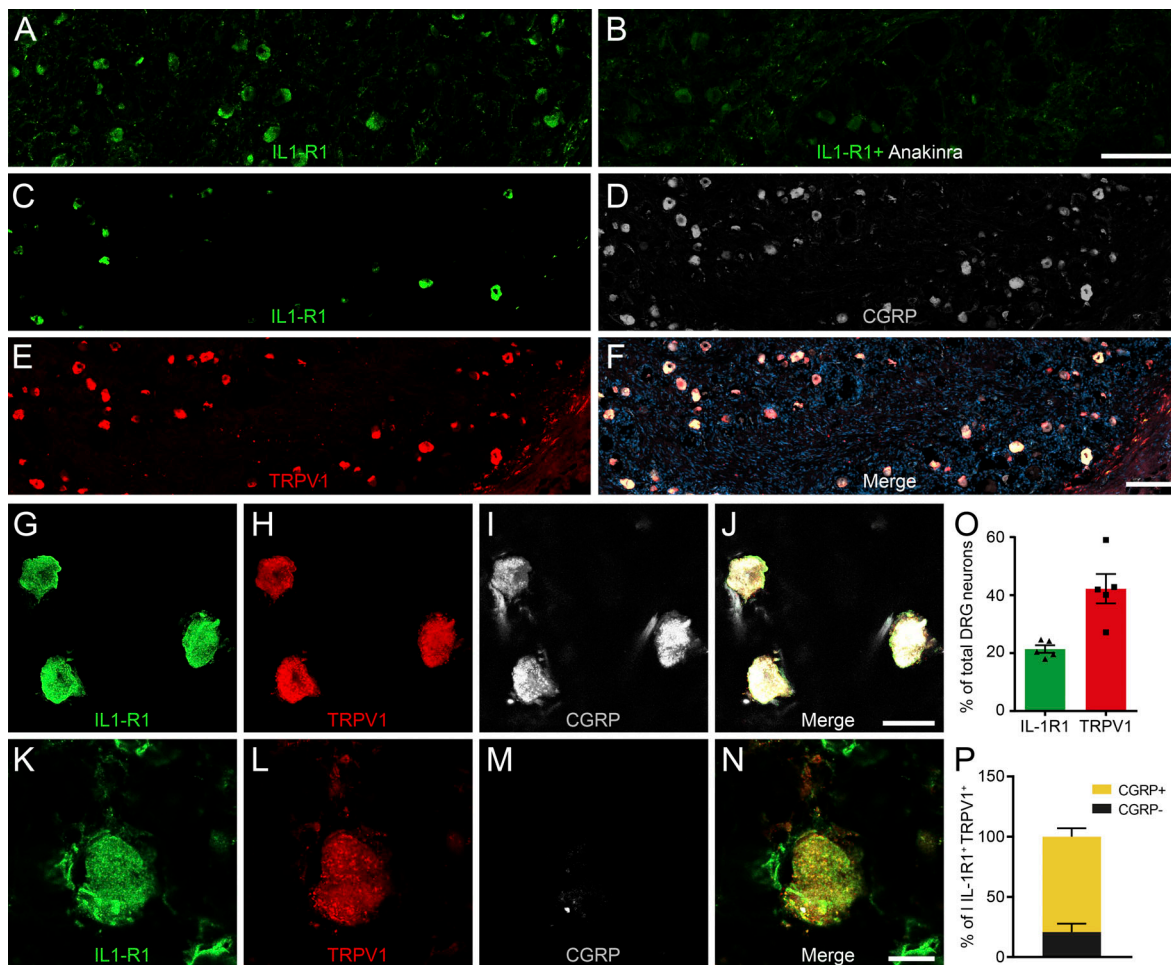


**Figure 5. IL-1R1 is expressed by NP TRPV1<sup>+</sup> sensory neurons of human DRGs.** (A and B) Validation of the specificity of the anti-IL-1R1 antibody by the absence of IL-1R1 immunostaining in fresh frozen human DRG sections preincubated with the blocking agent anakinra. (C–N) Immunofluorescence confocal microscopy of a postmortem human lumbar DRG immunostained for IL-1R1 (C, G, and K), TRPV1 (E, H, and L), and CGRP (D, I, and M). (O) Quantification of the relative number of DRG neurons expressing IL-1R1 and TRPV1. Data are expressed as a percentage of the total HuC/D<sup>+</sup> neuronal population in lumbar DRGs and represent means  $\pm$  SEM of five individuals. (P) The expression of CGRP was assessed in the total IL-1R1<sup>+</sup> TRPV1<sup>+</sup> double-positive subpopulation (set at 100%). Data are shown as mean  $\pm$  SEM. Scale bars: 200  $\mu$ m (B and F); 25  $\mu$ m (J); and 12.5  $\mu$ m (N).

deficits in both *Trpv1*<sup>Cre::Il1r1<sup>fl/fl</sup> mice and their WT littermates (Fig. 7 B). Accordingly, we found no gross difference between *Trpv1*<sup>Cre::Il1r1<sup>fl/fl</sup> and WT mice with respect to leukocyte infiltration in the spinal cord (Fig. 7, C–E). Despite the fact that *Trpv1*<sup>Cre::Il1r1<sup>fl/fl</sup> mice exhibit an EAE similar to that of their WT counterparts, *Trpv1*<sup>Cre::Il1r1<sup>fl/fl</sup> mice were resistant to allodynia development (Fig. 7 F). The allodynic response was assessed until the onset of EAE, a time that precedes the appearance of the first signs of paralysis, which would impair the animal’s ability to respond to tactile stimuli. These results indicate that the pain associated with this preclinical model of MS is caused in part by the activation of IL-1R1<sup>+</sup> nociceptors.</sup></sup></sup></sup>

We next determined whether the contribution of IL-1R1<sup>+</sup> nociceptors to pain transmission is specific to EAE or is common to a range of chronic inflammatory diseases. For that purpose, *Trpv1*<sup>Cre::Il1r1<sup>fl/fl</sup> conditional knockout mice were used in the K/BxN serum transfer model of inflammatory arthritis (Boilard et al., 2010). Similar to what we observed in EAE, we found that *Trpv1*<sup>Cre::Il1r1<sup>fl/fl</sup> and WT mice developed arthritis with a</sup></sup>

comparable time course and severity (Fig. 8, A and B). Furthermore, the recruitment of immune cells in the arthritic ankle joint of *Trpv1*<sup>Cre::Il1r1<sup>fl/fl</sup> mice was unaltered compared with WT mice (Fig. 8, C–E). However, *Trpv1*<sup>Cre::Il1r1<sup>fl/fl</sup> mice developed significantly less mechanical allodynia than WT mice between days 2 and 5 after K/BxN serum injection (Fig. 8 F), time points that preceded the peak of arthritis disease (i.e., days 6–7). Taken together with the finding that myeloid cells producing IL-1 $\beta$  massively infiltrated the arthritic mouse hind limbs (Fig. 2), this result suggests that the IL-1 $\beta$ /IL-1R1 axis plays a key role in the development of pain in inflammatory arthritis.</sup></sup>

We next asked whether this mechanism could be essential in an autoimmune-independent diseases such as OA. We found no differences in the extent of cartilage damage and disease progression between WT, *Il1r1*<sup>-/-</sup>, and *Trpv1*<sup>Cre::Il1r1<sup>fl/fl</sup> mice following intra-articular injection of mono-iodoacetate (MIA) in the knee (Fig. 9, A–C). However, when subjected to the knee-bend test during the course of OA, *Il1r1*<sup>-/-</sup> mice had significantly less movement-evoked pain than WT mice at 2, 3, and 4 wk after</sup>

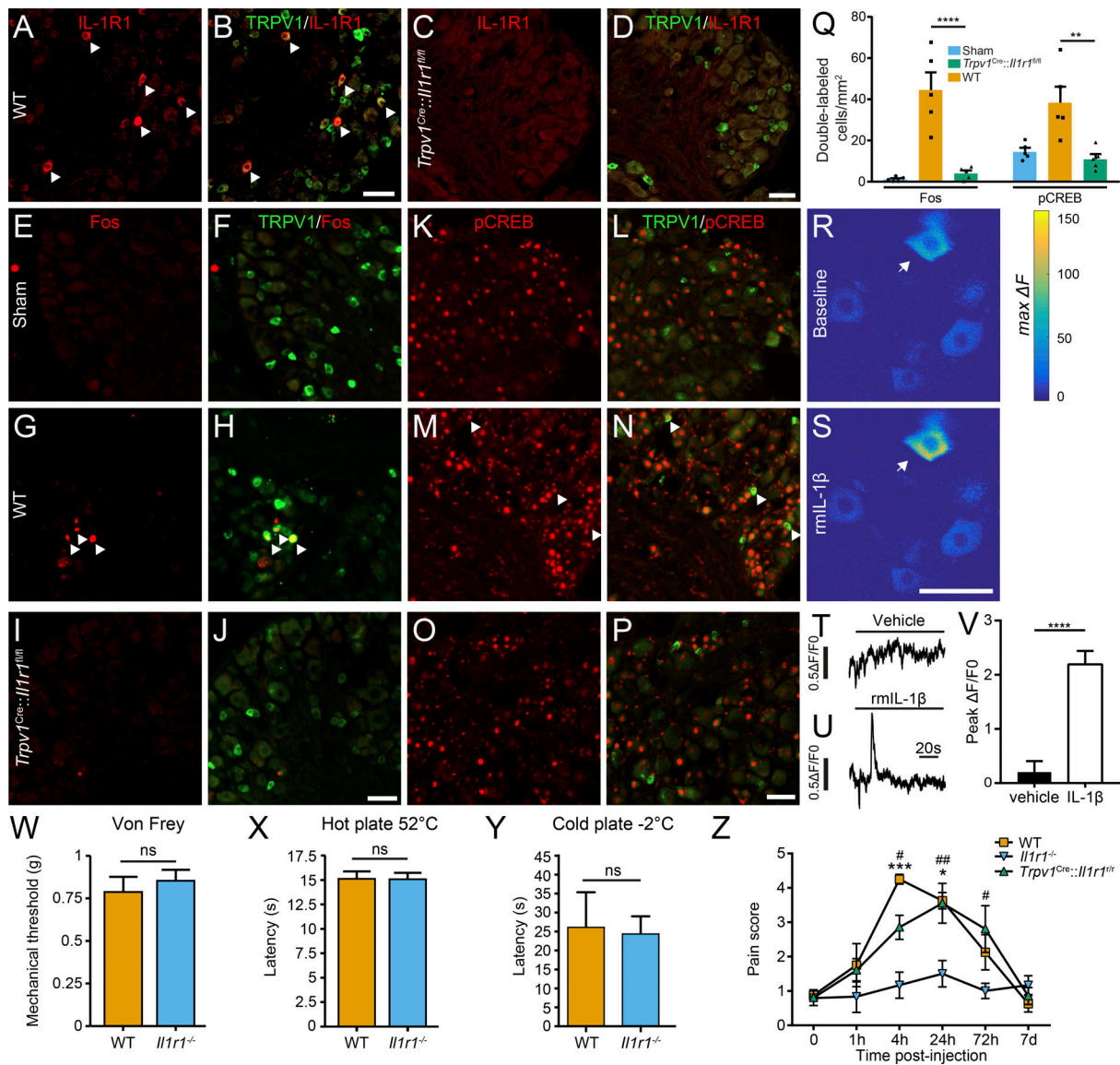


**Figure 6. IL-1 $\beta$  activation of IL-1R1 in TRPV1 $^+$  sensory neurons induces pain-related behavior in mice.** (A–D) Representative confocal images showing the specificity of the *Trpv1*<sup>Cre::</sup>*Il1r1*<sup>fl/fl</sup> mouse line, as demonstrated by the loss of IL-1R1 immunoreactivity (red signal) in TRPV1 $^+$  neurons (green) of *Trpv1*<sup>Cre::</sup>*Il1r1*<sup>fl/fl</sup> mice (C and D) compared with their WT littermates (A and B). (E–P) WT (G, H, M, and N) and *Trpv1*<sup>Cre::</sup>*Il1r1*<sup>fl/fl</sup> (I, J, O, and P) mice were injected unilaterally in the sciatic nerve with rmlL-1 $\beta$  and killed at 4 h after injection to assess expression in the L4–L6 DRGs of the cellular activation markers Fos (E–J) in red and pCREB (K–P) in red) in TRPV1 $^+$  sensory neurons (green). Sham animals (E, F, K, and L) received the same surgery but without injection. White arrowheads point to double-labeled neurons. (Q) Total counts of Fos $^+$  TRPV1 $^+$  cells and pCREB $^+$  TRPV1 $^+$  cells are reported as a function of the total tissue area (in millimeter squared;  $n = 5$  tissue sections per mouse, five mice per group). *Trpv1*<sup>WT/WT::</sup>*Il1r1*<sup>fl/fl</sup> mice were used as WT controls in A–Q. (R–V) The calcium response was measured in L4/L5 DRG neurons by means of in vivo video-rate two-photon functional imaging after direct application of rmlL-1 $\beta$  to the exposed DRG. Representative examples of neuronal responses (indicated by the arrows) after application of either vehicle or rmlL-1 $\beta$  are depicted as color-coded heatmaps of a typical imaging field (R and S) or as Ca $^{2+}$  curves (T and U). Quantification showing the significant calcium response to rmlL-1 $\beta$  over the vehicle treatment is shown in V ( $n = 4$  mice). (W–Y) Assessment of the nociceptive response to mechanical (W) and thermal (X and Y) stimuli in *Il1r1*<sup>-/-</sup> mice ( $n = 13$ ) compared with WT mice ( $n = 7$ ). (Z) Pain was assessed using the knee-bend test in WT ( $n = 4$ ), *Il1r1*<sup>-/-</sup> ( $n = 6$ ), and *Trpv1*<sup>Cre::</sup>*Il1r1*<sup>fl/fl</sup> ( $n = 10$ ) mice following intra-articular injection of rmlL-1 $\beta$  in the knee. C57BL/6 mice served as control mice in W–Y, whereas *Trpv1*<sup>WT/WT::</sup>*Il1r1*<sup>WT/WT</sup> mice were used as WT controls in Z. Data are shown as mean  $\pm$  SEM. Statistical significance was determined by a  $t$  test (V–Y) or by one-way (Q) or two-way repeated measures (Z) ANOVA followed by a Bonferroni post hoc test. \*,  $P < 0.05$ ; \*\*,  $P < 0.01$ ; \*\*\*,  $P < 0.001$ ; \*\*\*\*,  $P < 0.0001$ ; compared with the WT group (Q), vehicle treatment (V), or the *Il1r1*<sup>-/-</sup> group (Z). #,  $P < 0.05$ ; ##,  $P < 0.01$ ; *Il1r1*<sup>-/-</sup> mice compared with *Trpv1*<sup>Cre::</sup>*Il1r1*<sup>fl/fl</sup> mice (Z). Scale bars: 50  $\mu$ m (B); 50  $\mu$ m (D); 50  $\mu$ m (J); 50  $\mu$ m (P); and 50  $\mu$ m (S). ns, not significant.

MIA injection (Fig. 9, D and E). Importantly, transgenic restoration of IL-1R1 specifically in nociceptors using *Trpv1*<sup>Cre::</sup>*Il1r1*<sup>fl/fl</sup> mice restored pain sensitivity thresholds to the levels seen in WT mice. This finding suggests a predominant role for IL-1 $\beta$  in

the pain symptoms associated with OA. Altogether, our results demonstrate that neutralizing IL-1R1 in DRG nociceptors could help prevent associated pain symptoms in a diversity of chronic inflammatory diseases.

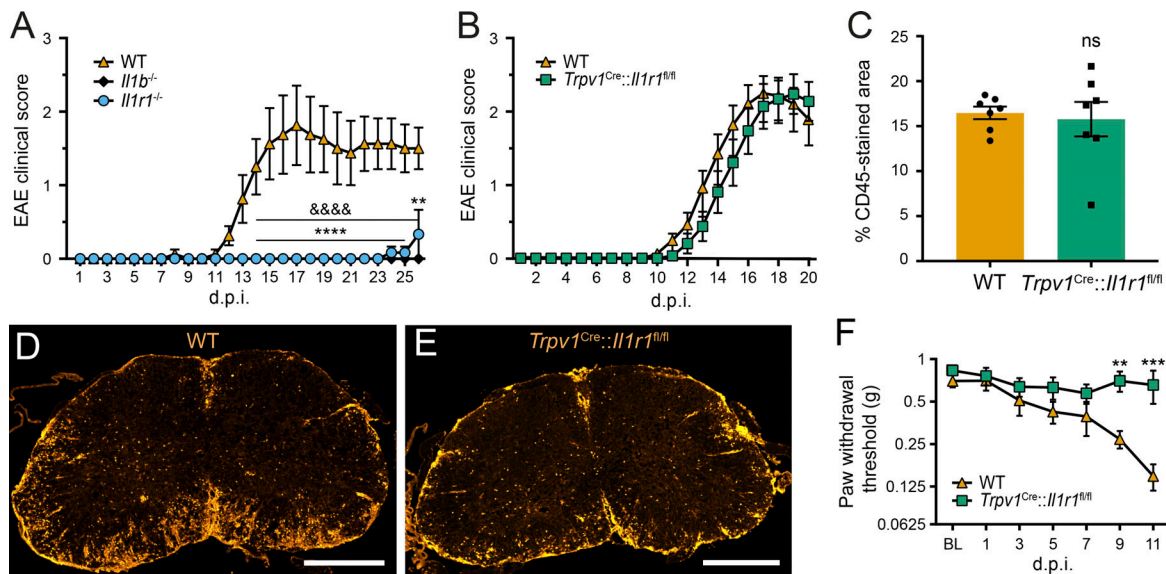


**Figure 7. IL-1R1 deficiency in nociceptors prevents the development of pain without affecting signs of inflammation and paralysis in EAE mice.** (A and B) The clinical course of MOG<sub>35-55</sub>-induced EAE was analyzed in mice constitutively lacking IL-1 $\beta$  ( $n = 10$ ) or IL-1R1 ( $n = 7$ , A;  $n = 14$ , B), mice with conditional deletion of IL-1R1 in TRPV1-expressing cells ( $Trpv1^{Cre::Il1r1^{fl/fl}}$  mice,  $n = 16$ ), and their respective WT control group ( $n = 10$ , A;  $n = 16$ , B). C57BL/6 mice served as WT controls in A, whereas  $Trpv1^{WT/WT::Il1r1^{fl/fl}}$  mice were used as WT mice in B–F. (C) Quantification of leukocyte infiltration as determined by immunodetection of the CD45 pan-leukocyte marker in the spinal cord of WT and  $Trpv1^{Cre::Il1r1^{fl/fl}}$  mice at 21 d after immunization (d.p.i.;  $n = 7$  mice/group). (D and E) Representative photomicrographs showing CD45 immunostaining in the spinal cord of EAE mice. (F) The development of mechanical allodynia was assessed using von Frey filaments in the two groups following EAE immunization ( $n = 16$ –24 mice/group; two independent experiments were pooled). Data are shown as mean  $\pm$  SEM. Statistical significance was determined by two-way (C) or two-way repeated-measures (A, B, and F) ANOVA followed by a Bonferroni post hoc test. \*\*,  $P < 0.01$ ; \*\*\*,  $P < 0.001$ ; \*\*\*\*,  $P < 0.0001$ ;  $Il1r1^{-/-}$  mice compared with the WT group in A. &&&&,  $P < 0.0001$ ;  $Il1b^{-/-}$  mice compared with the WT group in A. \*\*,  $P < 0.01$ ; \*\*\*,  $P < 0.001$ ;  $Trpv1^{Cre::Il1r1^{fl/fl}}$  mice compared with the WT group in B and F. Data in B and F are representative of two independent pooled experiments. Scale bars: 500  $\mu$ m (D and E). BL, baseline; ns, not significant.

## Discussion

The chronic production of IL-1 $\beta$  in inflammatory diseases such as MS/EAE, RA, and OA is one of the key factors involved in their pathogenesis. Accordingly, inhibition of the cellular sources of IL-1 $\beta$  has been postulated to be an effective therapeutic target for these diseases. The main contribution of IL-1 $\beta$  in these conditions is thought to be mediated through the mobilization of immune cells and the licensing of a pathogenic inflammatory signature. However, our results collected in mice with MS-like disease and arthritis revealed a cellular proximity between IL-1 $\beta$ -producing protagonists and their yet-to-be-studied axonal IL-1R1 target at the site of inflammation, whose stimulation leads to the rapid activation of IL-1R1-expressing nociceptors. The fact that IL-1 $\beta$  can directly affect TRPV1<sup>+</sup> nociceptors to induce and stimulate pain in inflammatory diseases was established using nociceptor-specific knockout and restored mouse lines. Finally, we provide evidence that this mechanism of inflammation-induced mechanical allodynia is likely shared by humans, as they express the same receptor machinery in their sensory neurons.

IL-1 $\beta$  expression by macrophages and neutrophils has long been recognized as occurring in various inflammatory conditions. However, despite interest in measuring IL-1 $\beta$  levels as a biomarker of disease severity, little attention has been paid to its nonimmune cell targets and nonclassical roles. This is in part due to the lack of proper tools available to specifically assess the expression of IL-1R1 and, in the present case, the difficulties

pertaining to the study of DRG sensory projections. Recently, new tools have enabled the imaging of the entire transparent rodent body and its three-dimensional reconstruction (Cai et al., 2019), which made possible the visualization of whole-body neuronal projections in adult fluorescent transgenic mice, even in the smallest tissues innervated by the peripheral nervous system. Some of these imaging tools were used here to show that IL-1 $\beta$ -producing myeloid cells are recruited next to IL-1R1<sup>+</sup> nociceptors during EAE and RA. This is an important observation, as the involvement of neurons in autoimmune inflammatory diseases remains elusive, and their response to inflammatory mediators is debated in the literature (Cook et al., 2018). The observed proximity between IL-1 $\beta$ -producing innate inflammatory cells and IL-1R1<sup>+</sup> neuronal processes indicates that it may be possible to develop a local treatment aimed at neutralizing the source, the target, or both, thus generating a completely different outcome. For example, in the case of an infection, controlling pain independently of inflammation would be desirable. In the inflammatory conditions tested in the present study, we report that IL-1 $\beta$  is predominantly produced by myeloid cells. We did not detect expression of IL-1 $\beta$  in glial satellite cells in the DRGs. However, we do not rule out that these cells could produce IL-1 $\beta$  in other inflammatory conditions, for example, following activation of toll-like receptors or tissue damage (Watkins and Maier, 2002).

Until now, the effect of inflammation on DRG neuron sensitization in animal models of inflammatory pain was assessed

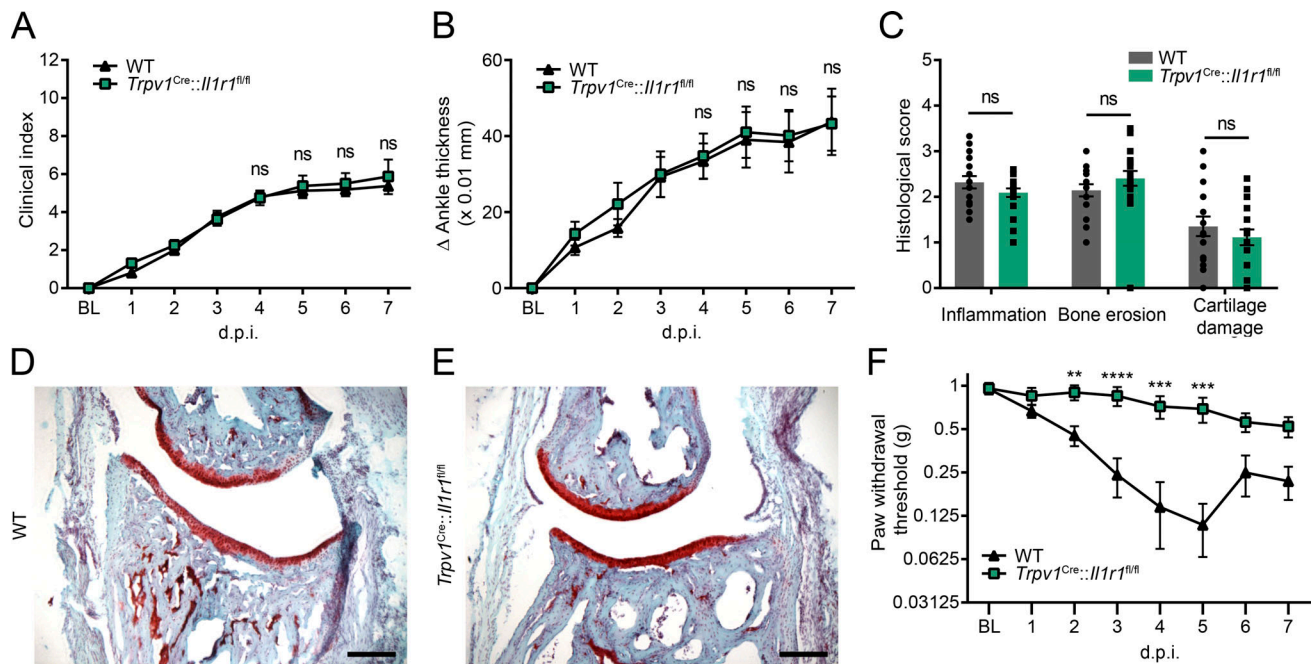


**Figure 8. Deletion of the *Il1r1* gene from nociceptors prevents allodynia without affecting ankle inflammation and swelling in the K/BxN arthritis model.** (A and B) The clinical course (A) and signs of arthritis (B) were monitored in mice with conditional deletion of IL-1R1 in TRPV1-expressing cells and their WT control mice ( $n = 16$  mice/group; two independent experiments were pooled). (C) Quantification of safranin-O staining in the arthritic ankle of *Trpv1<sup>Cre::Il1r1<sup>fl/fl</sup></sup>* and WT mice at 7 d after K/BxN serum injection ( $n = 10$  mice/group). (D and E) Representative examples of histochemical staining (safranin-O/hematoxylin/Fast green) showing the overall cytoarchitecture of articular cartilage of the tibiotalar joint at day 7. (F) The development of mechanical allodynia was assessed in arthritic *Trpv1<sup>Cre::Il1r1<sup>fl/fl</sup></sup>* and WT mice at various times after K/BxN serum transfer ( $n = 16$  mice/group; two independent experiments). *Trpv1<sup>WT/WT::Il1r1<sup>fl/fl</sup></sup>* mice were used as WT controls in A–F. Data are shown as mean  $\pm$  SEM. Statistical significance was determined using a one-way (C) or two-way repeated-measures (A, B, and F) ANOVA followed by a Bonferroni post hoc test. \*\*,  $P < 0.01$ ; \*\*\*,  $P < 0.001$ ; \*\*\*\*,  $P < 0.0001$  compared with the WT group. Scale bars: 200  $\mu$ m (D and E). Abbreviations: BL, baseline; d.p.i., days postinjection; ns, not significant.

mainly through the study of the TRPV1 receptor (Arima et al., 2015; Brandt et al., 2012; Chakrabarti et al., 2018). However, an innovative concept was recently introduced by Arima et al., who suggested that the DRGs, through their role in relaying information from the periphery to the CNS and their physical connection with the spinal cord, might provide an entry point for immune cells to the CNS during EAE (Arima et al., 2012; Arima et al., 2015). It was also shown that TRPV1<sup>+</sup> neurons, following stimulation with the specific TRPV1 agonist capsaicin, are able to induce central neurogenic inflammation, resulting in EAE relapse. Whether TRPV1 agonists promote or inhibit inflammation has, however, remained controversial. For example, TRPV1-knockout mice exhibited higher lethality in the peak phase of EAE but improved recovery in the chronic phase of disease (Musumeci et al., 2011). Treatment with the novel TRPV1 agonist SA13353 was found to reduce the production of proinflammatory cytokines and the severity of symptoms in mouse models of RA and EAE (for review, see Tsuji and Aono, 2012). Perhaps a better way to directly tackle inflammatory pain in autoimmune diseases would be to target IL-1R1 rather than TRPV1, which we know is expressed by a heterogeneous pool of DRG sensory neurons.

There are discrepancies in the literature regarding IL-1R1 expression by neurons and the effect that IL-1 $\beta$  has on them. Our data demonstrate that IL-1R1-expressing neurons comprise ~10% of the total lumbar DRG neuronal population. This finding

is coherent with data from a recent single-cell transcriptomic analysis of adult mouse lumbar DRG neurons (Usoskin et al., 2015) in which 9% of the DRG neurons interrogated expressed the *Il1r1* gene. Another transcriptomic study failed to detect IL-1R1 expression on enriched DRG nociceptors isolated using a magnetic purification approach (Thakur et al., 2014). However, the design of the latter study was based on the identification of nociceptor-enriched genes through comparison with the gene expression profile of dissociated whole ganglia, which likely means that genes expressed in small populations of neurons were underestimated. A recent study using a transgenic mouse line in which a fluorescent reporter was driven by the *Il1r1* promoter also failed to detect IL-1R1 in DRG neurons (Song et al., 2018). This discrepancy between their results and the study of Usoskin et al. (2015) and ours could be explained by the low protein turnover of IL-1R1 in neurons under unstressed conditions, resulting in an underestimation of IL-1R1 protein levels using a transcription-based approach. Importantly, the demonstration here that the IL-1R1 protein is abundantly expressed by human DRGs not only corroborates previous scRNA-seq studies performed in both mice and humans (Ray et al., 2018; Usoskin et al., 2015), but extends them by supporting the translational potential of targeting IL-1R1 to prevent pain. Still, one has to keep in mind that IL-1R1 expression may change under pathological conditions and that expression and function of IL-1R may not be the same in all types of sensory neurons.

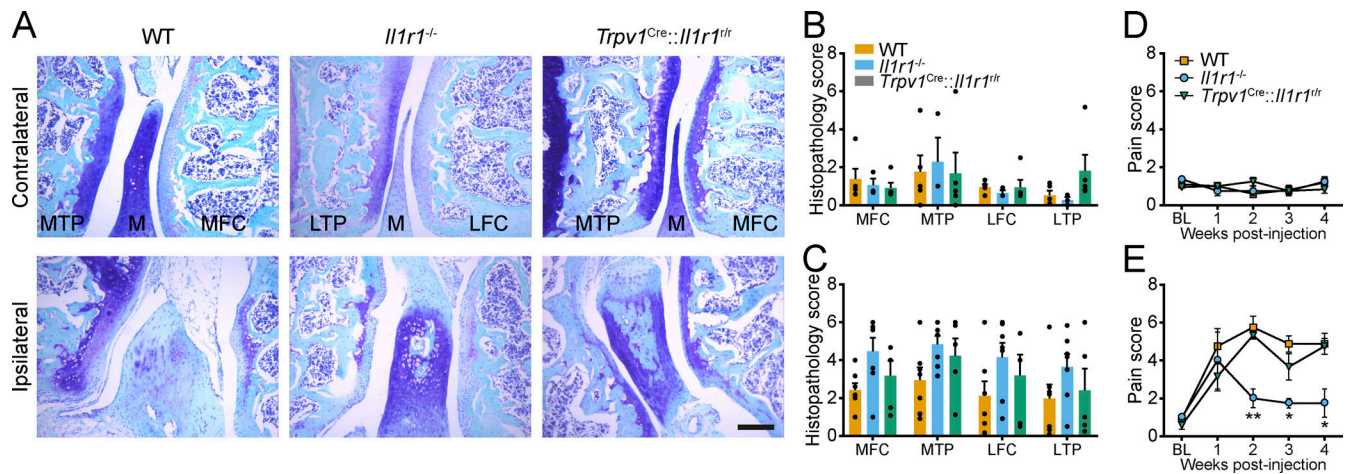


**Figure 9. Restoration of the *Il1r1* gene in nociceptors induces allodynia without affecting knee joint damage in the MIA OA model. (A–C)** Representative photomicrographs of histological sections of the knee joint of WT ( $n = 6$ ), *Il1r1<sup>-/-</sup>* ( $n = 7$ ), and *Trpv1<sup>Cre::</sup>Il1r1<sup>fl/fl</sup>* ( $n = 5$ ) mice at 4 wk after injection of MIA. Tissue sections were stained with Toluidine blue and Fast green to identify the articular cartilage, and cartilage damage was quantified in the main structures of the knee joint in both the ipsilateral (B) and contralateral (C) knee. **(D and E)** Mechanical allodynia assessment in the contralateral (D) and ipsilateral (E) knee joint following intra-articular injection of MIA in WT ( $n = 6$ ), *Il1r1<sup>-/-</sup>* ( $n = 7$ ), and *Trpv1<sup>Cre::</sup>Il1r1<sup>fl/fl</sup>* ( $n = 5$ ) mice. *Trpv1<sup>WT/WT::</sup>Il1r1<sup>WT/WT</sup>* mice were used as WT controls in A–E. Data are shown as mean  $\pm$  SEM. Statistical significance was determined by two-way (B and C) or two-way repeated-measures (D and E) ANOVA followed by a Bonferroni post hoc test. \*,  $P < 0.05$ ; \*\*,  $P < 0.01$ ; *Il1r1<sup>-/-</sup>* mice compared with the other two groups. BL, baseline; LFC, lateral femoral condyle; LTP, lateral tibial plateau; M, meniscus; MFC, medial femoral condyle; MTP, medial tibial plateau. Scale bar: 200  $\mu$ m (A).

The contribution of myeloid cells, such as macrophages and neutrophils, to the development of pain after peripheral nerve injury has been supported by a number of cell depletion studies in mice (Liu et al., 2000; Nadeau et al., 2011). Although the role of these innate immune cells in pain has been well established, the mechanisms by which they stimulate nociceptors are not well understood. We previously reported that mice lacking the proinflammatory cytokines IL-1 $\beta$  and TNF or their type 1 receptors (IL-1R1 and TNFR1) have reduced nociceptive sensitivity after peripheral nerve injury (Liu et al., 2000; Nadeau et al., 2011). Similarly, intrathecal administration of anakinra, a naturally occurring antagonist of IL-1R1, in combination with soluble TNF receptor exhibited an anti-allodynic effect in a rat L5 spinal nerve transection model of neuropathic pain (Sweitzer et al., 2001). Intraneural injection of recombinant forms of IL-1 $\beta$  and TNF into the rodent sciatic nerve induced thermal hyperalgesia and mechanical allodynia (Zelenka et al., 2005). However, it remains unclear whether IL-1 $\beta$  and TNF can directly modulate nociception by acting on sensory neurons or whether they indirectly affect pain via the recruitment of innate immune cells at the site of inflammation, which in turn release pain-inducing mediators. Here, we showed that the presence of IL-1 $\beta$  in the sciatic nerve or DRG induces direct and fast activation of TRPV1<sup>+</sup> DRG sensory neurons, a process that precedes the infiltration of neutrophils and monocytes at the site of administration. Furthermore, we found that nociceptor activation in this model is dependent on IL-1R1 expression by TRPV1<sup>+</sup> neurons and that restoration of IL-1R1 expression in TRPV1<sup>+</sup> neurons of *Il1r1<sup>-/-</sup>* mice (via Cre recombination) is sufficient to restore pain sensitivity. These findings suggest that the local production of IL-1 $\beta$  can directly trigger pain through the activation of neuronal IL-1R1. However, it should be kept in mind that in the context of chronic inflammatory diseases, IL-1R1 may signal to pain in the

absence of an agonistic ligand by interacting with ion channels, as was suggested to occur for the IL-17 receptor in the context of chemotherapy-induced neuropathic pain (Luo et al., 2019).

Using a conditional gene knockout approach that enabled us to specifically block IL-1R1 signaling in neurons, we uncovered that neuronal IL-1R1 is required for mechanical allodynia induced in two of the most common autoimmune inflammatory diseases. Deficiency in neuronal IL-1R1 signaling did not compromise peripheral and CNS inflammation, tissue damage, or clinical symptoms (except pain) caused by either EAE or RA. This finding is in agreement with previous work from us and others that revealed that leukocyte and endothelial IL-1R1 are the two main targets associated with the development and amplification of the autoimmune inflammatory response (Lévesque et al., 2016; McCandless et al., 2009; Mufazalov et al., 2017; Paré et al., 2018). However, the possibility that DRG sensory neurons may be able to influence neuroinflammation during EAE remains a topic of debate, especially with the discovery that sensory nerve stimulation (via soleus muscles) triggers activation of an endothelial IL-6–chemokine (C-C motif) ligand 20 amplification loop, leading to the accumulation of leukocytes in the dorsal vein at the L5 level of the spinal cord (Arima et al., 2012). It is interesting to note that in EAE, the expression of IL-6 by radio-resistant cells is regulated by IL-1 $\beta$  produced by macrophages and neutrophils (Dumas et al., 2014). Thus, whether and how the IL-1 $\beta$ –IL-1R1 cytokine system fits into this concept of IL-6–mediated inflammation amplifier remains to be experimentally tested.

The idea of neurogenic inflammation was further substantiated by another provocative study by Arima et al. (2015), which showed that pain induced by the activation of TRPV1 neurons through the injection of capsaicin triggered EAE relapse in mice. This observation appears to conflict with our finding

that EAE disease course and severity are unaffected by the inhibition of pain in immunized *Trpv1<sup>Cre</sup>::Il1r1<sup>fl/fl</sup>* mice. One explanation for these differences could be that the initial immune attack of the mouse CNS did not require pain, despite causing it, but that the subsequent relapses were influenced by it. Future work will help unravel mechanisms underlying the possible relationship between IL-1R1 and other pain-associated receptors such as TRPV1 and Nav1.8.

Similar to EAE, the intricate relationship between IL-1 $\beta$  signaling and the development of RA is well recognized, as best demonstrated by the fact that IL-1 $\beta$ -targeted therapies have been successfully translated to the clinic (Dinarello et al., 2012). The efficacy and excellent safety profile of anakinra and canakinumab (a human anti-IL-1 $\beta$  monoclonal antibody) are reasons why these drugs are the first-line indication in the treatment of juvenile arthritis (Sota et al., 2019). We add to this body of work by demonstrating that blocking IL-1R1 signaling in mice can also relieve pain associated with RA. Because we did not observe any difference in disease initiation and its progression in *Trpv1<sup>Cre</sup>::Il1r1<sup>fl/fl</sup>* mice compared with their control counterparts, we argue that the presence of IL-1R1 in nociceptors does not contribute to the pathogenesis of RA. The results discussed above suggest that IL-1R1-targeted therapies might have dual effects on inflammation and pain. These findings warrant future research aimed at understanding whether different coreceptors and signaling pathways come into play.

In contrast to MS/EAE and RA, OA is not an autoimmune disease. Yet, excessive proinflammatory cytokine production is well known to occur in OA, with IL-1 $\beta$  among the most abundantly expressed in joints of OA patients (Melchiorri et al., 1998). Some studies that tested the efficacy of anti-IL-1 therapies in animal models of OA have, however, reported disappointing results regarding the potential benefit of such treatment on disease progression (Nasi et al., 2017; van Dalen et al., 2017), which could be explained by the diversity of the models and their association (or lack thereof) with inflammation. The impact on pain was also frequently overlooked in prior studies. Here, we used the MIA model of OA, which induces rapid cartilage degradation and pain as early as 1 wk after injection. We found that deficiency in IL-1R1 had no significant benefit on cartilage damage but prevented pain from developing. One must keep in mind, however, that human OA is an inflammatory disease that is more progressive than MIA and that inflammation is believed to play a central role in cartilage degeneration and joint destruction in patients. Thus, patients suffering from inflammation-driven OA may experience greater benefits than animal models following treatment with anti-IL-1 drugs. Along this line, a recent randomized phase 1 clinical trial revealed that lutikizumab, a human dual-variable domain immunoglobulin targeting both IL-1 $\alpha$  and IL-1 $\beta$ , reduces inflammation in OA patients (Wang et al., 2017). The future will tell whether anti-IL-1 therapies can prevent pain and treat inflammation-driven OA at the same time.

In summary, we demonstrated that IL-1R1 is expressed by a subset of DRG nociceptors in both mice and humans and that the projections and terminals of these sensory neurons are surrounded by IL-1 $\beta$ -producing immune cells during chronic inflammatory diseases such as EAE and RA. Importantly, the expression of IL-1R1 by TRPV1<sup>+</sup> nociceptors was demonstrated to

be required for pain to develop in mouse models of EAE, RA, and OA. Collectively, this work shows that the proinflammatory cytokine IL-1 $\beta$  can directly induce pain by activating a new nociceptive receptor, namely neuronal IL-1R1. Therapies aimed at blocking IL-1 $\beta$ /IL-1R1 signaling could therefore have a dual effect in chronic inflammatory diseases: attenuating inflammation and the subsequent tissue degeneration and concurrently preventing the manifestation of pain.

## Materials and methods

### Animals

A total of 170 male and female mice were used in this study. For EAE and OA experiments, both males and females were pooled in the groups, as no difference in the induction or severity of the disease had been observed. For the K/BxN serum transfer model, only males were used in the experiment as there is a reported sex bias in this model, with the females developing a less severe disease. C57BL/6 mice were purchased from The Jackson Laboratory or Charles River at 8–10 wk of age. Breeders for *Il1r1<sup>fl/fl</sup>* mice were obtained from Dr. Ning Quan (Ohio State University, Columbus, OH; Liu et al., 2015), *pIl1b-DsRed* transgenic mice from Dr. Akira Takashima (University of Toledo, Toledo, OH; Matsushima et al., 2010), and *Il1b<sup>-/-</sup>* mice from Dr. Y. Iwakura (University of Tokyo, Tokyo, Japan; Horai et al., 1998). *Trpv1<sup>Cre</sup>* (JAX stock #017769), *Il1r1<sup>fl/fl</sup>* (#028398), *Sst<sup>Cre</sup>* (#013044), and *Rosa26-tdTomato* (also known as Ai9 or RCL-tdT; #007905) transgenic mice were purchased from The Jackson Laboratory. All mouse lines were bred in-house at the Animal Facility of the CHU de Québec–Université Laval Research Center, Stanford Neurosciences Institute, or McGill University. WT littermates generated from heterozygous matings were used as controls according to the breeding scheme shown in Fig. S1. Mice had ad libitum access to food and water.

### EAE induction and clinical scoring

Mice were immunized by two s.c. injections of 100  $\mu$ g of myelin oligodendrocyte glycoprotein peptide 35–55 (MOG<sub>35–55</sub>; MEVGWYRSPFSRVVHLYRNGK; Feldan) emulsified in 100  $\mu$ l of incomplete Freund's adjuvant supplemented with 4 mg/ml heat-inactivated *Mycobacterium tuberculosis* H37Ra (BD Biosciences). Pertussis toxin (200 ng/mouse; List Biological Laboratories Inc.) was injected i.v. consecutive to MOG<sub>35–55</sub> injections and again 2 d later. Animals were monitored daily to assess weight loss and scored using a grading scale of 0 to 5, following recommendations of Stromnes and Goverman (2006): 0 = unaffected, 0.5 = partially limp tail, 1 = paralyzed tail, 1.5 = loss in coordinated movements, 2 = hind limb paresis, 2.5 = one hind limb paralyzed, 3 = both hind limbs paralyzed, 3.5 = hind limbs paralyzed and weakness in forelimbs, 4 = one forelimb paralyzed, 4.5 = both forelimbs paralyzed, and 5 = moribund/death. Mice displaying a score of  $\geq 2$  received daily manual bladder evacuation, and those with a score  $> 3.5$  received daily s.c. injections of sterile saline.

### Inflammatory arthritis induction and scoring

Inflammatory arthritis was induced using arthritogenic K/BxN serum (200  $\mu$ l), transferred by intraperitoneal injection to

recipient mice on experimental days 0 and 2. The development of arthritis was monitored daily by assessing the clinical index of arthritis, graded on a scale from 0 to 12, as previously described (Monach et al., 2007; Monach et al., 2010). Delta ankle thickness was measured at the malleoli, with the ankle in a fully flexed position, using a spring-loaded precision caliper (Käfer dial thickness gauge J15; Käfer Messuhrenfabrik GmbH & Co.).

### OA induction and scoring

The MIA model of OA was induced as previously described (He et al., 2017). Briefly, under isoflurane anesthesia, mice were injected intra-articularly with 5  $\mu$ l of MIA at a concentration of 50  $\mu$ g/ $\mu$ l diluted in physiological saline, with the needle passing behind the patellar ligament into the joint space of the left knee. Movement-induced behavioral reactions were assessed using the knee-bend test in both the ipsilateral knee (injected) and the contralateral knee, used as a measure of normal responsiveness according to the scoring scale developed by Ferreira-Gomes et al. (2008).

### Mechanical and thermal sensitivity assessment

Mechanical allodynia was measured by placing mice on an elevated wire-mesh grid and stimulating the plantar surface of the hind paw with a set of calibrated von Frey filaments (Stoelting) following our previously published method (Nadeau et al., 2011; Petitjean et al., 2015). Animals were habituated to the testing environment daily for at least a week before baseline testing. Before experimentation, mice were allowed to acclimatize for at least 1 h in individual plastic boxes with a wire mesh floor (Ugo Basile). In brief, calibrated von Frey filaments (ranging from 0.008 to 2.0 g) were applied to the plantar surface of each hind paw in ascending order of bending force by a blinded investigator. Each monofilament was applied five times per paw, and the number of nociceptive responses was recorded. The monofilament that produced nociceptive responses (paw withdrawal) >60% of the time was used to determine the mechanical nociceptive threshold, as described previously (Chaplan et al., 1994; Mills et al., 2012).

Thermal nocifensive behaviors to heat and cold were assessed as previously described (Bautista et al., 2007), using a Hot/Cold Plate (Bioseb) set at 52°C and -2°C, respectively. The time required to elicit a nocifensive response (latency), either paw lifting or paw shaking or licking, shivering, or jumping, was recorded for each animal following contact with the plate, with a maximum time limit of 30 s on the hot plate and 60 s on the cold plate to prevent paw pad injuries. Each animal was tested at least three times for both temperatures, with a minimum 5-min interval between tests.

### Injection of IL-1 $\beta$

For intraneural sciatic nerve injections, mice were anesthetized under isoflurane, and the left sciatic nerve was surgically exposed. Microinjections of 100 ng of carrier-free rmIL-1 $\beta$  (PreproTech) diluted in sterile PBS were made through a pulled-glass micropipette (30- $\mu$ m external diameter) connected to a 5- $\mu$ l Hamilton syringe. Treatment consisted of two microinjections of 0.5  $\mu$ l each (1  $\mu$ l total) into the two major branches

of the sciatic nerve. For the knee injection, mice were anesthetized under isoflurane and injected intra-articularly with 5  $\mu$ l of rmIL-1 $\beta$  at a concentration of 2 pg/ $\mu$ l diluted in physiological saline (10 pg total), with the needle passing behind the patellar ligament into the joint space of the left knee.

### In vivo DRG calcium imaging

*Trpv1*<sup>Cre</sup> mice transduced with the GCaMP6s virus were imaged as previously described (Wang et al., 2018). Briefly, *Trpv1*<sup>Cre</sup> heterozygous mice at postnatal day 3 to postnatal day 6 of age were injected s.c. with an adeno-associated virus 9 (AAV9) harboring Cre-inducible GCaMP6s under the control of a CAG promoter with expression enhanced by WPRE sequence (AAV9.CAG.Flex.GCaMP6s.WPRE.SV40; Addgene; 100842-AAV9). In total, 5  $\mu$ l of the virus (with a titer >1  $\times$  10<sup>12</sup> vg/ml) was injected into the plantar area of the hind paw using a 25- $\mu$ l Hamilton syringe fitted with a 30G 1/2-gauge needle. Both hind paws were injected. Mice were imaged 6 to 8 wk after the injection. For functional imaging of calcium, a laminectomy was performed to expose L4 and L5 DRGs. Anesthetized mice were then fixed on a custom-made stabilization device, and Ca<sup>2+</sup> responses were recorded using a homemade video-rate two-photon microscope following application of rmIL-1 $\beta$  (100 ng) or vehicle directly to the exposed DRGs. In total, we recorded 968 neurons from 23 imaging fields of  $\sim$ 400  $\times$  200  $\mu$ m from four mice. A response was considered positive when the peak of the Ca<sup>2+</sup> trace ( $\Delta F/F_0$  curve) during rmIL-1 $\beta$  or vehicle application was above  $F_b + (F_{b-max} - F_b) \times x$ , where  $x$  was a value chosen between 2 and 3, depending on baseline stability, to ensure the most reliable detection.  $F_b$  and  $F_{b-max}$  were calculated as average and maximum  $\Delta F/F_0$  values during baseline before the application of vehicle or rmIL-1 $\beta$ , respectively.

### Immunostaining and histology

Mice were overdosed with ketamine-xylazine and transcardially perfused with PBS followed by 1% paraformaldehyde (vol/vol; pH 7.4). DRG and spinal cords were dissected out from vertebral columns, postfixed in 1% paraformaldehyde 48 h at 4°C, and then transferred into PBS + 20% sucrose for at least 24 h before tissue sectioning. To preserve the structural integrity of the dorsal roots, some spinal cords were left inside the vertebral columns, and a decalcification step was performed right after the post-fixation step by incubating in 0.5 M EDTA (pH 7.4) for 4 d under constant agitation, with a medium (decalcification solution) change after 2 d. The spinal cords enclosed in the backbone were then transferred for 1 d into a PBS + 20% sucrose solution and embedded in Shandon M-1 Embedding Matrix (Thermo Fisher Scientific) before sectioning. Depending on the experimental protocol, DRGs and lumbar spinal cord segments were cut at a thickness of 12 and 14  $\mu$ m, respectively, using a cryostat (Leica Biosystems).

Immunofluorescence labeling was performed according to our previously published method (de Rivero Vaccari et al., 2012). Primary antibodies used in this study are from the following sources (catalog numbers in parentheses) and were used at the indicated dilutions: guinea pig anti-TRPV1 (also known as capsaicin receptor; 1:1,000; Millipore; AB5566), rabbit anti-TRPV1

(1:500; Alomone Labs; ACC-030), biotin-conjugated lectin from *Bandeiraea simplicifolia* (1:1,000; Sigma-Aldrich; L2140), rat anti-CD31 (1:1,000; BD Biosciences; 557355), goat anti-Iba-1 (1:1,500; Novus Biochemical; NB100-1028), goat anti-IL-1R1 (1:100; R&D Systems; AF-771), goat anti-IL-1 $\beta$  (1:100; R&D Systems; AF-401NA), mouse anti-NeuN (1:250; Millipore; MAB377), mouse anti-HuC/D (1:100; Invitrogen; A6455), rabbit anti-laminin (1:1,000; Dako; Z0097), mouse anti-CGRP (1:1,000; Abcam; ab81887), rabbit anti-P2X3 (1:2,000; Abcam; ab10269), rat anti-Ly6G (1:2,000; BD Biosciences; 551459), rabbit anti-Fos (1:500; Cell Signaling Technology; 2250), rabbit anti-pCREB (1:500; Cell Signaling Technology; 9198), rat anti-CD45 (1:750; BD Biosciences; 553076), and mouse anti-TH (1:1,000; Millipore; MAB318). Secondary antibodies conjugated to DyLight 405 (1:100; Jackson ImmunoResearch Laboratories; 715-475-151) or Alexa Fluor (1:200; Life Technologies Corp.), and streptavidin (which binds to biotin) conjugated to Alexa Fluor 647 (1:1,000; Thermo Fisher Scientific; S21374) were used as secondary and tertiary antibodies, whereas DAPI (1  $\mu$ g/ml; Life Technologies Corp.) was used for nuclear counterstaining. For the blocking of anti-IL-1R1 antibody binding sites, fresh frozen human DRG sections were preincubated with anakinra (Kineret; 150 mg/ml, 1:25 dilution) before incubation with the anti-IL-1R1 primary antibody. Sections were imaged on a Zeiss LSM 800 confocal microscope system equipped with 405-nm, 488-nm, 561-nm, and 640-nm lasers or Zeiss Axio Scan.Z1 slide scanner equipped with a Colibri 2 LED source. Confocal images were acquired using a Zeiss Axiocam 506 Mono Camera and mosaics created using the Zen 2.3 software (Blue edition).

### Quantitative analyses

For the quantitative assessment of cell numbers in tissue sections prepared from the DRGs, spinal nerve roots, and ankle joints, the analysis was performed on the digitized whole-tissue sections acquired using a Zeiss Slide Scanner Axio Scan.Z1 at 20 $\times$  magnification. All cell counts were performed using Fiji software (version 1.52h, National Institutes of Health [NIH]; Schindelin et al., 2012). Briefly, a grid was overlaid on the tissue area of interest, and the Cell Counter tool in Fiji was used to manually count (and classify) cells according to their protein expression profile. Only cells with a DAPI-stained nucleus were counted. Data were expressed as the average number of positive cells per millimeter squared of tissue section or the percentage of cells that expressed specific markers, and at least five tissue sections per animal were analyzed. For the quantitative evaluation of inflammation in the spinal cord, the proportional area of tissue immunostained for CD45 within the entire coronal section was measured using images taken with the Zeiss Slide Scanner Axio Scan.Z1. Thresholding values in Fiji were chosen such that only labeled product resulted in measurable pixels on the digitized images. Contrast between positive signal and background was maximized and held constant between all images. Data were expressed as the proportional area of the spinal cord cross section occupied by immunostaining, and at least three tissue sections per animal were quantified. All quantifications were performed blind with respect to the identity of the animals.

For the histomorphometric analysis of the ankle joint in the K/BxN serum transfer arthritis model, tissue sections were

processed as described above for the spinal cord (with a decalcification of 1 wk in 0.5 M EDTA) and stained with Safranin O, hematoxylin, and Fast green (Lorenz et al., 2014). The sections were digitized using an Axio Scan.Z1 slide scanner, and histological scoring was performed for both the tibiotalar and talonavicular joints by a blinded investigator, using the previously described criteria (Chen et al., 2006; Pettit et al., 2001). At least four tissue sections per animal were quantified for each joint. The scores of both joints were averaged and used as the individual animal score.

For the histopathological analysis of the articular cartilage in OA mice, paraffin-embedded mid-coronal sections (8- $\mu$ m-thick) of the ipsilateral and contralateral knees were stained with Toluidine blue and Fast green and scored as described before (Glass et al., 1993; He et al., 2017).

### Human tissues

Human DRGs were obtained from the NIH Neurobiobank (University of Maryland, Baltimore, MD). The five tested sample tissues were harvested from a 51-yr-old white female who died of atherosclerotic cardiovascular disease; a 66-yr-old female who died in a car accident; a 41-yr-old male who died of atherosclerotic cardiovascular disease; a 48-yr-old white male who died of hypertensive atherosclerotic cardiovascular disease; and a 65-yr-old white male who died of atherosclerotic cardiovascular disease. None of the subjects had reported inflammatory-related comorbidities or CNS diseases, thus classifying them as unaffected controls for this study.

### Bioinformatic analysis of RNA-seq data

The bioinformatic analysis was performed using the publicly available scRNA-seq database generated from adult mouse DRG neurons (Zeisel et al., 2018), using raw sequence data deposited at the National Center for Biotechnology Information Sequence Read Archive under accession no. SRX3809270. Briefly, scRNA-seq reads provided for each DRG subpopulation were aligned against the neuropeptides listed in the NeuroPep database (Wang et al., 2015) and those annotated with gene ontology (GO) terms “neuropeptide signaling pathway” (GO:0007218), “neuropeptide binding” (GO:0042923), and “neuropeptide receptor binding” (GO:0071855).

### Statistics

Statistical evaluations were performed using one- or two-way ANOVA or repeated-measures ANOVA where appropriate. The multiple comparisons adjustment was made using the Bonferroni correction. All statistical analyses were performed using GraphPad Prism software (v.7). A P value <0.05 was considered statistically significant. All data in the graphs are expressed as means  $\pm$  SEM.

### Study approval

Experiments were approved by the Animal Welfare Committees of Université Laval and McGill University, in accordance with the Canadian Council on Animal Care policy or Stanford University’s Administrative Panel on Laboratory Animal Care. Postmortem human DRGs were obtained from the NIH

Neurobiobank and used under local ethical approval (#2012-1138) by the Comité d'éthique de la recherche du CHU de Québec-Université Laval.

### Online supplemental material

**Fig. S1** shows a schematic representation of the breeding strategy used in the present study to generate cell-specific IL-1R1 restored and knockout mouse lines. **Table S1** lists the differentially expressed genes associated with neuropeptides, neuromodulators, and neurotransmitters among the different DRG neuronal subtypes using scRNA-seq raw data from [Zeisel et al. \(2018\)](#).

### Acknowledgments

We thank Nicolas Vallières, Nadia Fortin, Martine Lessard, Tania Lévesque, and Martine Saint-Pierre for their invaluable technical assistance.

This study was supported by grants from the Multiple Sclerosis Society of Canada (EGID-2446 and EGID-3587 to S. Lacroix), Canadian Institutes of Health Research (PJT-168852 to S. Lacroix, MOP-130471 to R. Sharif-Naeini), Natural Sciences and Engineering Research Council of Canada (RGPIN-2015-05281 to S. Lacroix, RGPIN-436091-13 to R. Sharif-Naeini), NIH (R01NS106301 and R01DA044481 to G. Scherrer), Department of Defense Neurosensory Research Award (MR130053 to G. Scherrer), and New York Stem Cell Foundation (to G. Scherrer). E. Boilard is the recipient of an investigator award from the Canadian Institutes of Health Research. F. Cicchetti is supported by a Research Chair from the Fonds de Recherche du Québec – Santé (FRQS). G. Scherrer is a New York Stem Cell Foundation Robertson Investigator. Salary support to B. Mailhot and R. Turmel was provided by FRQS. Salary support to M. Christin was provided by a Postdoctoral Fellowship from the Louise and Alan Edwards Foundation. N. Tessandier is the recipient of a doctoral studentship from the Arthritis Society and FRQS. Salary support to F. Bretheau was in part provided by the Fondation du CHU de Québec and the Centre thématique de recherche en neurosciences.

Author contributions: B. Mailhot conceived the study, designed and performed most of the experiments, analyzed the data, prepared the figures, and wrote the manuscript. M. Christin induced OA, performed histopathology scoring, and measured mechanical allodynia in knockout mice. N. Tessandier induced arthritis and scored the degree of inflammation and swelling in knockout mice. C. Sotoudeh, R. Turmel, and É. Pellerin performed immunofluorescence, acquired microscopy images, and performed quantitative analyses of some of the data in Fig. 3. F. Bretheau provided intellectual input on the project and commented on the manuscript. F. Wang performed in vivo video-rate two-photon calcium imaging and commented on the manuscript. C. Bories provided guidance related to calcium imaging experiments and commented on the manuscript. C. Joly-Beauparlant performed RNA-seq data extraction and bioinformatic analysis. F. Cicchetti provided human tissue and commented on the manuscript. A. Droit provided guidance related to bioinformatic analysis and commented on the

manuscript. Y. De Koninck provided the mouse model and expertise with calcium functional imaging. G. Scherrer provided some mouse models and guidance related to the characterization of IL-1R1<sup>+</sup> DRG sensory neurons, as well as commented on the manuscript. E. Boilard helped design the arthritis experiments, provided input in the data analysis, and commented on the manuscript. R. Sharif-Naeini provided input related to pain and OA experiments and commented on the manuscript. S. Lacroix conceived the study, designed the experiments, supervised the overall project, and wrote the manuscript.

Disclosures: The authors declare no competing interests exist.

Submitted: 2 August 2019

Revised: 3 March 2020

Accepted: 13 May 2020

### References

- Allan, S.M., P.J. Tyrrell, and N.J. Rothwell. 2005. Interleukin-1 and neuronal injury. *Nat. Rev. Immunol.* 5:629–640. <https://doi.org/10.1038/nri1664>
- Arima, Y., M. Harada, D. Kamimura, J.H. Park, F. Kawano, F.E. Yull, T. Kawamoto, Y. Iwakura, U.A. Betz, G. Márquez, et al. 2012. Regional neural activation defines a gateway for autoreactive T cells to cross the blood-brain barrier. *Cell.* 148:447–457. <https://doi.org/10.1016/j.cell.2012.01.022>
- Arima, Y., D. Kamimura, T. Atsumi, M. Harada, T. Kawamoto, N. Nishikawa, A. Stofkova, T. Ohki, K. Higuchi, Y. Morimoto, et al. 2015. A pain-mediated neural signal induces relapse in murine autoimmune encephalomyelitis, a multiple sclerosis model. *eLife.* 4. e08733. <https://doi.org/10.7554/eLife.08733>
- Aubé, B., S.A. Lévesque, A. Paré, É. Chamma, H. Kébir, R. Gorina, M.A. Lécuyer, J.I. Alvarez, Y. De Koninck, B. Engelhardt, et al. 2014. Neutrophils mediate blood-spinal cord barrier disruption in demyelinating neuroinflammatory diseases. *J. Immunol.* 193:2438–2454. <https://doi.org/10.4049/jimmunol.1400401>
- Balasingam, V., T. Tejada-Berges, E. Wright, R. Bouckova, and V.W. Yong. 1994. Reactive astrogliosis in the neonatal mouse brain and its modulation by cytokines. *J. Neurosci.* 14:846–856. <https://doi.org/10.1523/JNEUROSCI.14-02-00846.1994>
- Bautista, D.M., J. Siemens, J.M. Glazer, P.R. Tsuruda, A.I. Basbaum, C.L. Stucky, S.E. Jordt, and D. Julius. 2007. The menthol receptor TRPM8 is the principal detector of environmental cold. *Nature.* 448:204–208. <https://doi.org/10.1038/nature05910>
- Binshtok, A.M., H. Wang, K. Zimmermann, F. Amaya, D. Vardeh, L. Shi, G.J. Brenner, R.R. Ji, B.P. Bean, C.J. Woolf, et al. 2008. Nociceptors are interleukin-1beta sensors. *J. Neurosci.* 28:14062–14073. <https://doi.org/10.1523/JNEUROSCI.3795-08.2008>
- Boilard, E., P.A. Nigrovic, K. Larabee, G.F. Watts, J.S. Cobllyn, M.E. Weinblatt, E.M. Massarotti, E. Remold-O'Donnell, R.W. Farndale, J. Ware, et al. 2010. Platelets amplify inflammation in arthritis via collagen-dependent microparticle production. *Science.* 327:580–583. <https://doi.org/10.1126/science.1181928>
- Bölcskei, K., Z. Helyes, A. Szabó, K. Sándor, K. Elekes, J. Németh, R. Almási, E. Pintér, G. Petho, and J. Szolcsányi. 2005. Investigation of the role of TRPV1 receptors in acute and chronic nociceptive processes using gene-deficient mice. *Pain.* 117:368–376. <https://doi.org/10.1016/j.pain.2005.06.024>
- Borbély, É., B. Botz, K. Bölskei, T. Kenyér, L. Kereskai, T. Kiss, J. Szolcsányi, E. Pintér, J.Z. Csepregi, A. Mócsai, et al. 2015. Capsaicin-sensitive sensory nerves exert complex regulatory functions in the serum-transfer mouse model of autoimmune arthritis. *Brain Behav. Immun.* 45:50–59. <https://doi.org/10.1016/j.bbi.2014.12.012>
- Brandt, M.R., C.E. Beyer, and S.M. Stahl. 2012. TRPV1 Antagonists and Chronic Pain: Beyond Thermal Perception. *Pharmaceuticals (Basel).* 5: 114–132. <https://doi.org/10.3390/ph5020114>
- Bruttger, J., K. Karram, S. Wörtge, T. Regen, F. Marini, N. Hoppmann, M. Klein, T. Blank, S. Yona, Y. Wolf, et al. 2015. Genetic Cell Ablation Reveals Clusters of Local Self-Renewing Microglia in the Mammalian

- Central Nervous System. *Immunity*. 43:92–106. <https://doi.org/10.1016/j.immuni.2015.06.012>
- Cai, R., C. Pan, A. Ghasemigharagoz, M.I. Todorov, B. Förstera, S. Zhao, H.S. Bhatia, A. Parra-Damas, L. Mrowka, D. Theodorou, et al. 2019. Panoptic imaging of transparent mice reveals whole-body neuronal projections and skull-meninges connections. *Nat. Neurosci.* 22:317–327. <https://doi.org/10.1038/s41593-018-0301-3>
- Chakrabarti, S., L.A. Pattison, K. Singhal, J.R.F. Hockley, G. Callejo, and E.S.J. Smith. 2018. Acute inflammation sensitizes knee-innervating sensory neurons and decreases mouse digging behavior in a TRPV1-dependent manner. *Neuropharmacology*. 143:49–62. <https://doi.org/10.1016/j.neuropharm.2018.09.014>
- Chaplan, S.R., F.W. Bach, J.W. Pogrel, J.M. Chung, and T.L. Yaksh. 1994. Quantitative assessment of tactile allodynia in the rat paw. *J. Neurosci. Methods*. 53:55–63. [https://doi.org/10.1016/0165-0270\(94\)90144-9](https://doi.org/10.1016/0165-0270(94)90144-9)
- Chen, M., B.K. Lam, Y. Kanaoka, P.A. Nigrovic, L.P. Audoly, K.F. Austen, and D.M. Lee. 2006. Neutrophil-derived leukotriene B4 is required for inflammatory arthritis. *J. Exp. Med.* 203:837–842. <https://doi.org/10.1084/jem.20052371>
- Christianson, C.A., M. Corr, G.S. Firestein, A. Mobargha, T.L. Yaksh, and C.I. Svensson. 2010. Characterization of the acute and persistent pain state present in K/BxN serum transfer arthritis. *Pain*. 151:394–403. <https://doi.org/10.1016/j.pain.2010.07.030>
- Cohen, S.B., L.W. Moreland, J.J. Cush, M.W. Greenwald, S. Block, W.J. Shergy, P.S. Hanrahan, M.M. Kraishi, A. Patel, G. Sun, et al.; 990145 Study Group. 2004. A multicentre, double blind, randomised, placebo controlled trial of anakinra (Kineret), a recombinant interleukin 1 receptor antagonist, in patients with rheumatoid arthritis treated with background methotrexate. *Ann. Rheum. Dis.* 63:1062–1068. <https://doi.org/10.1136/ard.2003.016014>
- Cook, A.D., A.D. Christensen, D. Tewari, S.B. McMahon, and J.A. Hamilton. 2018. Immune Cytokines and Their Receptors in Inflammatory Pain. *Trends Immunol.* 39:240–255. <https://doi.org/10.1016/j.it.2017.12.003>
- de Rivero Vaccari, J.P., D. Bastien, G. Yurcisin, I. Pineau, W.D. Dietrich, Y. De Koninck, R.W. Keane, and S. Lacroix. 2012. P2X4 receptors influence inflammasome activation after spinal cord injury. *J. Neurosci.* 32:3058–3066. <https://doi.org/10.1523/JNEUROSCI.4930-11.2012>
- Dinarelo, C.A., A. Simon, and J.W. van der Meer. 2012. Treating inflammation by blocking interleukin-1 in a broad spectrum of diseases. *Nat. Rev. Drug Discov.* 11:633–652. <https://doi.org/10.1038/nrd3800>
- Dumas, A., N. Amiable, J.P. de Rivero Vaccari, J.J. Chae, R.W. Keane, S. Lacroix, and L. Vallières. 2014. The inflammasome pyrin contributes to pertussis toxin-induced IL-1 $\beta$  synthesis, neutrophil intravascular crawling and autoimmune encephalomyelitis. *PLoS Pathog.* 10:e1004150. <https://doi.org/10.1371/journal.ppat.1004150>
- Ferreira-Gomes, J., S. Adães, and J.M. Castro-Lopes. 2008. Assessment of movement-evoked pain in osteoarthritis by the knee-bend and CatWalk tests: a clinically relevant study. *J. Pain*. 9:945–954. <https://doi.org/10.1016/j.jpain.2008.05.012>
- Glass, J.D., T.M. Brushart, E.B. George, and J.W. Griffin. 1993. Prolonged survival of transected nerve fibres in C57BL/Ola mice is an intrinsic characteristic of the axon. *J. Neurocytol.* 22:311–321. <https://doi.org/10.1007/BF01195555>
- Goldberg, D.S., and S.J. McGee. 2011. Pain as a global public health priority. *BMC Public Health*. 11:770. <https://doi.org/10.1186/1471-2458-11-770>
- He, B.H., M. Christin, S. Mouchbahani-Constance, A. Davidova, and R. Sharif-Naeini. 2017. Mechanosensitive ion channels in articular nociceptors drive mechanical allodynia in osteoarthritis. *Osteoarthritis Cartilage*. 25:2091–2099. <https://doi.org/10.1016/j.joca.2017.08.012>
- Horai, R., M. Asano, K. Sudo, H. Kanuka, M. Suzuki, M. Nishihara, M. Takahashi, and Y. Iwakura. 1998. Production of mice deficient in genes for interleukin (IL)-1 $\alpha$ , IL-1 $\beta$ , IL-1 $\alpha$ / $\beta$ , and IL-1 receptor antagonist shows that IL-1 $\beta$  is crucial in turpentine-induced fever development and glucocorticoid secretion. *J. Exp. Med.* 187:1463–1475. <https://doi.org/10.1084/jem.187.9.1463>
- Huang, Y., D.E. Smith, O. Ibáñez-Sandoval, J.E. Sims, and W.J. Friedman. 2011. Neuron-specific effects of interleukin-1 $\beta$  are mediated by a novel isoform of the IL-1 receptor accessory protein. *J. Neurosci.* 31:18048–18059. <https://doi.org/10.1523/JNEUROSCI.4067-11.2011>
- Jenei-Lanzl, Z., A. Meurer, and F. Zaucke. 2019. Interleukin-1 $\beta$  signaling in osteoarthritis - chondrocytes in focus. *Cell. Signal.* 53:212–223. <https://doi.org/10.1016/j.cellsig.2018.10.005>
- Ji, H., A. Pettit, K. Ohmura, A. Ortiz-Lopez, V. Duchatelle, C. Degott, E. Gravalles, D. Mathis, and C. Benoist. 2002. Critical roles for interleukin 1 and tumor necrosis factor alpha in antibody-induced arthritis. *J. Exp. Med.* 196:77–85. <https://doi.org/10.1084/jem.20020439>
- Kawasaki, Y., L. Zhang, J.K. Cheng, and R.R. Ji. 2008. Cytokine mechanisms of central sensitization: distinct and overlapping role of interleukin-1 $\beta$ , interleukin-6, and tumor necrosis factor- $\alpha$  in regulating synaptic and neuronal activity in the superficial spinal cord. *J. Neurosci.* 28:5189–5194. <https://doi.org/10.1523/JNEUROSCI.3338-07.2008>
- Kelly, S., R.J. Chapman, S. Woodhams, D.R. Sagar, J. Turner, J.J. Burston, C. Bullock, K. Paton, J. Huang, A. Wong, et al. 2015. Increased function of pronociceptive TRPV1 at the level of the joint in a rat model of osteoarthritis pain. *Ann. Rheum. Dis.* 74:252–259. <https://doi.org/10.1136/annrheumdis-2013-203413>
- Koda, K., K. Hyakkoku, K. Ogawa, K. Takasu, S. Imai, Y. Sakurai, M. Fujita, H. Ono, M. Yamamoto, I. Fukuda, et al. 2016. Sensitization of TRPV1 by protein kinase C in rats with mono-iodoacetate-induced joint pain. *Osteoarthritis Cartilage*. 24:1254–1262. <https://doi.org/10.1016/j.joca.2016.02.010>
- Lacroix, S., L. Vallières, and S. Rivest. 1996. C-fos mRNA pattern and corticotropin-releasing factor neuronal activity throughout the brain of rats injected centrally with a prostaglandin of E2 type. *J. Neuroimmunol.* 70:163–179. [https://doi.org/10.1016/S0165-5728\(96\)00114-2](https://doi.org/10.1016/S0165-5728(96)00114-2)
- Lévesque, S.A., A. Paré, B. Mailhot, V. Bellver-Landete, H. Kébir, M.A. Lécuyer, J.L. Alvarez, A. Prat, J.P. de Rivero Vaccari, R.W. Keane, et al. 2016. Myeloid cell transmigration across the CNS vasculature triggers IL-1 $\beta$ -driven neuroinflammation during autoimmune encephalomyelitis in mice. *J. Exp. Med.* 213:929–949. <https://doi.org/10.1084/jem.20151437>
- Li, Q., N. Powell, H. Zhang, N. Belevych, S. Ching, Q. Chen, J. Sheridan, C. Whitacre, and N. Quan. 2011. Endothelial IL-1R1 is a critical mediator of EAE pathogenesis. *Brain Behav. Immun.* 25:160–167. <https://doi.org/10.1016/j.bbi.2010.09.009>
- Liu, X., and N. Quan. 2018. Microglia and CNS Interleukin-1: Beyond Immunological Concepts. *Front. Neurol.* 9:8. <https://doi.org/10.3389/fneur.2018.00008>
- Liu, T., N. van Rooijen, and D.J. Tracey. 2000. Depletion of macrophages reduces axonal degeneration and hyperalgesia following nerve injury. *Pain*. 86:25–32. [https://doi.org/10.1016/S0304-3959\(99\)00306-1](https://doi.org/10.1016/S0304-3959(99)00306-1)
- Liu, L., T.M. Yang, W. Liedtke, and S.A. Simon. 2006. Chronic IL-1 $\beta$  signaling potentiates voltage-dependent sodium currents in trigeminal nociceptive neurons. *J. Neurophysiol.* 95:1478–1490. <https://doi.org/10.1152/jn.00509.2005>
- Liu, X., T. Yamashita, Q. Chen, N. Belevych, D.B. Mckim, A.J. Tarr, V. Coppola, N. Nath, D.P. Nemeth, Z.W. Syed, et al. 2015. Interleukin 1 type 1 receptor restore: a genetic mouse model for studying interleukin 1 receptor-mediated effects in specific cell types. *J. Neurosci.* 35:2860–2870. <https://doi.org/10.1523/JNEUROSCI.3199-14.2015>
- Liu, X., D.P. Nemeth, D.B. McKim, L. Zhu, D.J. DiSabato, O. Berdysz, G. Gorantla, B. Oliver, K.G. Witcher, Y. Wang, et al. 2019. Cell-Type-Specific Interleukin 1 Receptor 1 Signaling in the Brain Regulates Distinct Neuroimmune Activities. *Immunity*. 50:764–766. <https://doi.org/10.1016/j.immuni.2019.02.012>
- Lorenz, J., E. Seebach, G. Hackmayer, C. Greth, R.J. Bauer, K. Kleinschmidt, D. Bettenworth, M. Böhm, J. Grifka, and S. Grässel. 2014. Melanocortin 1 receptor-signaling deficiency results in an articular cartilage phenotype and accelerates pathogenesis of surgically induced murine osteoarthritis. *PLoS One*. 9:e105858. <https://doi.org/10.1371/journal.pone.0105858>
- Luo, H., H.Z. Liu, W.W. Zhang, M. Matsuda, N. Lv, G. Chen, Z.Z. Xu, and Y.Q. Zhang. 2019. Interleukin-17 Regulates Neuron-Glia Communications, Synaptic Transmission, and Neuropathic Pain after Chemotherapy. *Cell Rep.* 29:2384–2397.e5. <https://doi.org/10.1016/j.celrep.2019.10.085>
- Matsushima, H., Y. Ogawa, T. Miyazaki, H. Tanaka, A. Nishibu, and A. Takashima. 2010. Intravital imaging of IL-1 $\beta$  production in skin. *J. Invest. Dermatol.* 130:1571–1580. <https://doi.org/10.1038/jid.2010.11>
- McCandless, E.E., M. Budde, J.R. Lees, D. Dorsey, E. Lyng, and R.S. Klein. 2009. IL-1R signaling within the central nervous system regulates CXCL12 expression at the blood-brain barrier and disease severity during experimental autoimmune encephalomyelitis. *J. Immunol.* 183:613–620. <https://doi.org/10.4049/jimmunol.0802258>
- Melchiorri, C., R. Meliconi, L. Frizziero, T. Silvestri, L. Pulsatelli, I. Mazzetti, R.M. Borzi, M. Uguccioni, and A. Facchini. 1998. Enhanced and coordinated in vivo expression of inflammatory cytokines and nitric oxide synthase by chondrocytes from patients with osteoarthritis. *Arthritis Rheum.* 41:2165–2174. [https://doi.org/10.1002/1529-0131\(199812\)41:12<2165::AID-ART11>3.0.CO;2-0](https://doi.org/10.1002/1529-0131(199812)41:12<2165::AID-ART11>3.0.CO;2-0)
- Mertens, M., and J.A. Singh. 2009. Anakinra for rheumatoid arthritis. *Cochrane Database Syst. Rev.* (1). CD005121.

- Miffelin, K.A., and B.J. Kerr. 2017. Pain in autoimmune disorders. *J. Neurosci. Res.* 95:1282–1294. <https://doi.org/10.1002/jnr.23844>
- Mills, C., D. Leblond, S. Joshi, C. Zhu, G. Hsieh, P. Jacobson, M. Meyer, and M. Decker. 2012. Estimating efficacy and drug ED50's using von Frey thresholds: impact of weber's law and log transformation. *J. Pain.* 13: 519–523. <https://doi.org/10.1016/j.jpain.2012.02.009>
- Monach, P., K. Hattori, H. Huang, E. Hyatt, J. Morse, L. Nguyen, A. Ortiz-Lopez, H.J. Wu, D. Mathis, and C. Benoist. 2007. The K/BxN mouse model of inflammatory arthritis: theory and practice. *Methods Mol. Med.* 136:269–282. [https://doi.org/10.1007/978-1-59745-402-5\\_20](https://doi.org/10.1007/978-1-59745-402-5_20)
- Monach, P.A., P.A. Nigrovic, M. Chen, H. Hock, D.M. Lee, C. Benoist, and D. Mathis. 2010. Neutrophils in a mouse model of autoantibody-mediated arthritis: critical producers of Fc receptor gamma, the receptor for C5a, and lymphocyte function-associated antigen 1. *Arthritis Rheum.* 62: 753–764. <https://doi.org/10.1002/art.27238>
- Mufazalov, I.A., C. Schelmbauer, T. Regen, J. Kuschmann, F. Wanke, L.A. Gabriel, J. Hauptmann, W. Müller, E. Pinteaux, F.C. Kurschus, et al. 2017. IL-1 signaling is critical for expansion but not generation of autoreactive GM-CSF<sup>+</sup> Th17 cells. *EMBO J.* 36:102–115. <https://doi.org/10.15252/embj.201694615>
- Musumeci, G., G. Grasselli, S. Rossi, V. De Chiara, A. Musella, C. Motta, V. Studer, G. Bernardi, N. Haji, H. Sepman, et al. 2011. Transient receptor potential vanilloid 1 channels modulate the synaptic effects of TNF- $\alpha$  and of IL-1 $\beta$  in experimental autoimmune encephalomyelitis. *Neurobiol. Dis.* 43:669–677. <https://doi.org/10.1016/j.nbd.2011.05.018>
- Nadeau, S., M. Filali, J. Zhang, B.J. Kerr, S. Rivest, D. Soulet, Y. Iwakura, J.P. de Rivero Vaccari, R.W. Keane, and S. Lacroix. 2011. Functional recovery after peripheral nerve injury is dependent on the pro-inflammatory cytokines IL-1 $\beta$  and TNF: implications for neuropathic pain. *J. Neurosci.* 31:12533–12542. <https://doi.org/10.1523/JNEUROSCI.2840-11.2011>
- Nasi, S., H.K. Ea, A. So, and N. Busso. 2017. Revisiting the Role of Interleukin-1 Pathway in Osteoarthritis: Interleukin-1 $\alpha$  and -1 $\beta$ , and NLRP3 Inflammasome Are Not Involved in the Pathological Features of the Murine Menisectomy Model of Osteoarthritis. *Front. Pharmacol.* 8:282. <https://doi.org/10.3389/fphar.2017.00282>
- Nigrovic, P.A., B.A. Binstadt, P.A. Monach, A. Johnsen, M. Gurish, Y. Iwakura, C. Benoist, D. Mathis, and D.M. Lee. 2007. Mast cells contribute to initiation of autoantibody-mediated arthritis via IL-1. *Proc. Natl. Acad. Sci. USA.* 104:2325–2330. <https://doi.org/10.1073/pnas.0610852103>
- Olechowski, C.J., J.J. Truong, and B.J. Kerr. 2009. Neuropathic pain behaviours in a chronic-relapsing model of experimental autoimmune encephalomyelitis (EAE). *Pain.* 141:156–164. <https://doi.org/10.1016/j.pain.2008.11.002>
- Paré, A., B. Mailhot, S.A. Lévesque, C. Juzwik, P.M. Ignatius Arokia Doss, M.A. Lécuyer, A. Prat, M. Rangachari, A. Fournier, and S. Lacroix. 2018. IL-1 $\beta$  enables CNS access to CCR2<sup>hi</sup> monocytes and the generation of pathogenic cells through GM-CSF released by CNS endothelial cells. *Proc. Natl. Acad. Sci. USA.* 115:E1194–E1203. <https://doi.org/10.1073/pnas.1714948115>
- Petitjean, H., S.A. Pawlowski, S.L. Fraine, B. Sharif, D. Hamad, T. Fatima, J. Berg, C.M. Brown, L.Y. Jan, A. Ribeiro-da-Silva, et al. 2015. Dorsal horn parvalbumin neurons are gate-keepers of touch-evoked pain after nerve injury. *Cell Rep.* 13:1246–1257. <https://doi.org/10.1016/j.celrep.2015.09.080>
- Pettit, A.R., H. Ji, D. von Stechow, R. Müller, S.R. Goldring, Y. Choi, C. Benoist, and E.M. Gravallese. 2001. TRANCE/RANKL knockout mice are protected from bone erosion in a serum transfer model of arthritis. *Am. J. Pathol.* 159:1689–1699. [https://doi.org/10.1016/S0002-9440\(10\)63016-7](https://doi.org/10.1016/S0002-9440(10)63016-7)
- Pietras, E.M., C. Mirantes-Barbeito, S. Fong, D. Loeffler, L.V. Kovtonyuk, S. Zhang, R. Lakshminarasimhan, C.P. Chin, J.M. Techner, B. Will, et al. 2016. Chronic interleukin-1 exposure drives haematopoietic stem cells towards precocious myeloid differentiation at the expense of self-renewal. *Nat. Cell Biol.* 18:607–618. <https://doi.org/10.1038/ncb3346>
- Ray, P., A. Torck, L. Quigley, A. Wangzhou, M. Neiman, C. Rao, T. Lam, J.Y. Kim, T.H. Kim, M.Q. Zhang, et al. 2018. Comparative transcriptome profiling of the human and mouse dorsal root ganglia: an RNA-seq-based resource for pain and sensory neuroscience research. *Pain.* 159: 1325–1345. <https://doi.org/10.1097/j.pain.0000000000001217>
- Schindelin, J., I. Arganda-Carreras, E. Frise, V. Kaynig, M. Longair, T. Pietzsch, S. Preibisch, C. Rueden, S. Saalfeld, B. Schmid, et al. 2012. Fiji: an open-source platform for biological-image analysis. *Nat. Methods.* 9: 676–682. <https://doi.org/10.1038/nmeth.2019>
- Segond von Banquet, G., C. König, J. Patzer, A. Eitner, J. Leuchtweis, M. Ebbinghaus, M.K. Boettger, and H.G. Schaible. 2016. Long-Lasting Activation of the Transcription Factor CREB in Sensory Neurons by Interleukin-1 $\beta$  During Antigen-Induced Arthritis in Rats: A Mechanism of Persistent Arthritis Pain? *Arthritis Rheumatol.* 68:532–541. <https://doi.org/10.1002/art.39445>
- Senger, J.L., K.M. Chan, H. Macandili, A.W.M. Chan, V.M.K. Verge, K.E. Jones, and C.A. Webber. 2019. Conditioning electrical stimulation promotes functional nerve regeneration. *Exp. Neurol.* 315:60–71. <https://doi.org/10.1016/j.expneurol.2019.02.001>
- Smith, D.E., B.P. Lipsky, C. Russell, R.R. Ketchum, J. Kirchner, K. Hensley, Y. Huang, W.J. Friedman, V. Boissonneault, M.M. Plante, et al. 2009. A central nervous system-restricted isoform of the interleukin-1 receptor accessory protein modulates neuronal responses to interleukin-1. *Immunity.* 30:817–831. <https://doi.org/10.1016/j.immuni.2009.03.020>
- Sofat, N., V. Ejindu, and P. Kiely. 2011. What makes osteoarthritis painful? The evidence for local and central pain processing. *Rheumatology (Oxford).* 50:2157–2165. <https://doi.org/10.1093/rheumatology/ker283>
- Song, A., L. Zhu, G. Gorantla, O. Berdysz, S.A. Amici, M. Guerau-de-Arellano, K.M. Madalena, J.K. Lerch, X. Liu, and N. Quan. 2018. Salient type 1 interleukin 1 receptor expression in peripheral non-immune cells. *Sci. Rep.* 8:723. <https://doi.org/10.1038/s41598-018-19248-7>
- Sota, J., A. Insalaco, R. Cimaz, M. Alessio, M. Cattalini, R. Gallizzi, M.C. Maggio, G. Lopalco, F. La Torre, C. Fabiani, et al. 2019. Drug Retention Rate and Predictive Factors of Drug Survival for Interleukin-1 Inhibitors in Systemic Juvenile Idiopathic Arthritis. *Front. Pharmacol.* 9:1526. <https://doi.org/10.3389/fphar.2018.01526>
- Stromnes, I.M., and J.M. Goverman. 2006. Active induction of experimental allergic encephalomyelitis. *Nat. Protoc.* 1:1810–1819. <https://doi.org/10.1038/nprot.2006.285>
- Sweitzer, S., D. Martin, and J.A. DeLeo. 2001. Intrathecal interleukin-1 receptor antagonist in combination with soluble tumor necrosis factor receptor exhibits an anti-allodynic action in a rat model of neuropathic pain. *Neuroscience.* 103:529–539. [https://doi.org/10.1016/S0306-4522\(00\)00574-1](https://doi.org/10.1016/S0306-4522(00)00574-1)
- Takeda, M., T. Tanimoto, J. Kadoi, M. Nasu, M. Takahashi, J. Kitagawa, and S. Matsumoto. 2007. Enhanced excitability of nociceptive trigeminal ganglion neurons by satellite glial cytokine following peripheral inflammation. *Pain.* 129:155–166. <https://doi.org/10.1016/j.pain.2006.10.007>
- Thakur, M., M. Crow, N. Richards, G.I. Davey, E. Levine, J.H. Kelleher, C.C. Agle, F. Denk, S.D. Harridge, and S.B. McMahon. 2014. Defining the nociceptor transcriptome. *Front. Mol. Neurosci.* 7:87. <https://doi.org/10.3389/fnmol.2014.00087>
- Tsuji, F., and H. Aono. 2012. Role of transient receptor potential vanilloid 1 in inflammation and autoimmune diseases. *Pharmaceuticals (Basel).* 5: 837–852. <https://doi.org/10.3390/ph5080837>
- Usoskin, D., A. Furlan, S. Islam, H. Abdo, P. Lönnnerberg, D. Lou, J. Hjerling-Leffler, J. Haegström, O. Kharchenko, P.V. Kharchenko, et al. 2015. Unbiased classification of sensory neuron types by large-scale single-cell RNA sequencing. *Nat. Neurosci.* 18:145–153. <https://doi.org/10.1038/nn.3881>
- van Dalen, S.C., A.B. Blom, A.W. Sløtjes, M.M. Helsen, J. Roth, T. Vogl, F.A. van de Loo, M.I. Koenders, P.M. van der Kraan, W.B. van den Berg, et al. 2017. Interleukin-1 is not involved in synovial inflammation and cartilage destruction in collagenase-induced osteoarthritis. *Osteoarthritis Cartilage.* 25:385–396. <https://doi.org/10.1016/j.joca.2016.09.009>
- Walder, R.Y., R. Radhakrishnan, L. Loo, L.A. Rasmussen, D.P. Mohapatra, S.P. Wilson, and K.A. Sluka. 2012. TRPV1 is important for mechanical and heat sensitivity in uninjured animals and development of heat hypersensitivity after muscle inflammation. *Pain.* 153:1664–1672. <https://doi.org/10.1016/j.pain.2012.04.034>
- Walsh, D.A., and D.F. McWilliams. 2014. Mechanisms, impact and management of pain in rheumatoid arthritis. *Nat. Rev. Rheumatol.* 10:581–592. <https://doi.org/10.1038/nrrheum.2014.64>
- Wang, Y., M. Wang, S. Yin, R. Jang, J. Wang, Z. Xue, and T. Xu. 2015. NeuroPep: a comprehensive resource of neuropeptides. *Database (Oxford).* 2015. bav038. <https://doi.org/10.1093/database/bav038>
- Wang, S.X., S.B. Abramson, M. Attur, M.A. Karsdal, R.A. Preston, C.J. Lozada, M.P. Kosloski, F. Hong, P. Jiang, M.J. Saltarelli, et al. 2017. Safety, tolerability, and pharmacodynamics of an anti-interleukin-1 $\alpha/\beta$  dual variable domain immunoglobulin in patients with osteoarthritis of the knee: a randomized phase 1 study. *Osteoarthritis Cartilage.* 25:1952–1961. <https://doi.org/10.1016/j.joca.2017.09.007>
- Wang, F., E. Bélanger, S.L. Côté, P. Desrosiers, S.A. Prescott, D.C. Côté, and Y. De Koninck. 2018. Sensory Afferents Use Different Coding Strategies for Heat and Cold. *Cell Rep.* 23:2001–2013. <https://doi.org/10.1016/j.celrep.2018.04.065>

- Watkins, L.R., and S.F. Maier. 2002. Beyond neurons: evidence that immune and glial cells contribute to pathological pain states. *Physiol. Rev.* 82: 981-1011. <https://doi.org/10.1152/physrev.00011.2002>
- Wojdasiewicz, P., L.A. Poniatowski, and D. Szukiewicz. 2014. The role of inflammatory and anti-inflammatory cytokines in the pathogenesis of osteoarthritis. *Mediators Inflamm.* 2014. 561459. <https://doi.org/10.1155/2014/561459>
- Yan, X., and H.R. Weng. 2013. Endogenous interleukin-1 $\beta$  in neuropathic rats enhances glutamate release from the primary afferents in the spinal dorsal horn through coupling with presynaptic N-methyl-D-aspartic acid receptors. *J. Biol. Chem.* 288:30544-30557. <https://doi.org/10.1074/jbc.M113.495465>
- Zeisel, A., H. Hochgerner, P. Lönnerberg, A. Johnsson, F. Memic, J. van der Zwan, M. Häring, E. Braun, L.E. Borm, G. La Manno, et al. 2018. Molecular Architecture of the Mouse Nervous System. *Cell.* 174: 999-1014.e22. <https://doi.org/10.1016/j.cell.2018.06.021>
- Zelenka, M., M. Schäfers, and C. Sommer. 2005. Intraneural injection of interleukin-1 $\beta$  and tumor necrosis factor- $\alpha$  into rat sciatic nerve at physiological doses induces signs of neuropathic pain. *Pain.* 116: 257-263. <https://doi.org/10.1016/j.pain.2005.04.018>

## Supplemental material

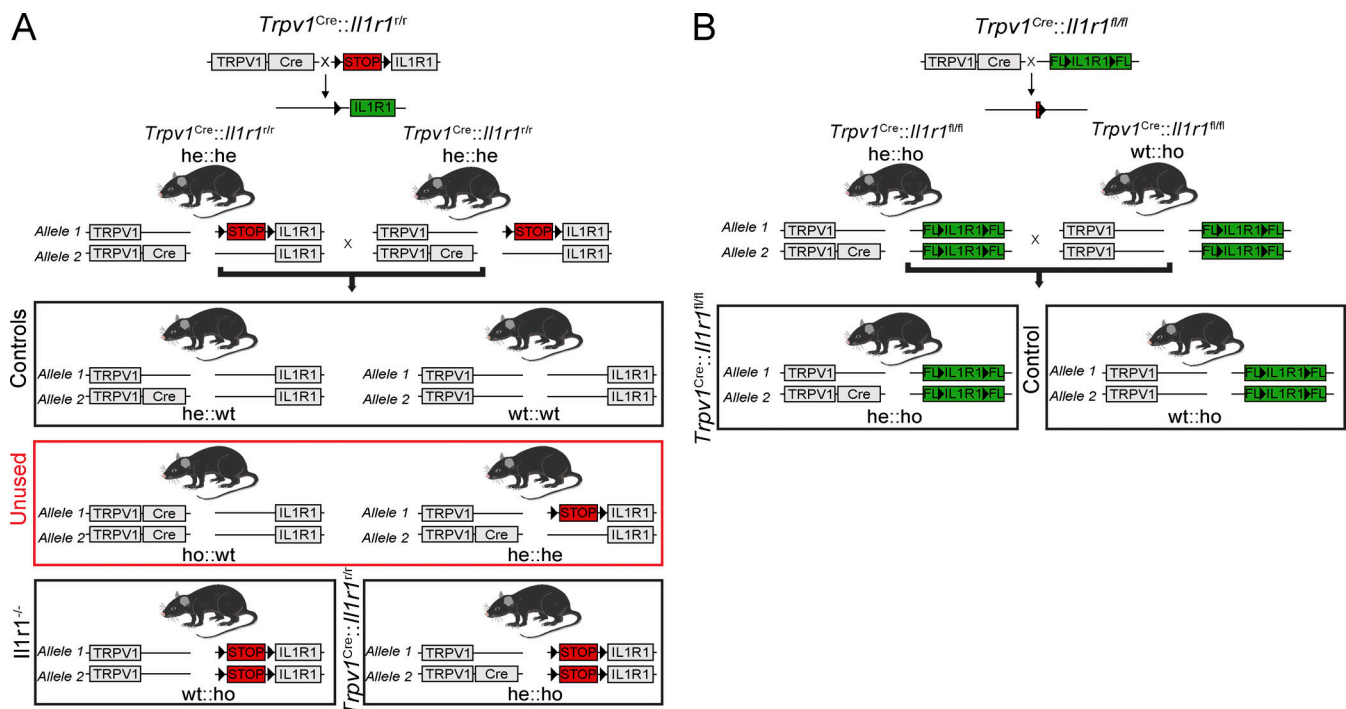


Figure S1. **Breeding strategy used to generate nociceptor-specific IL-1R1 restored and knockout mouse lines. (A and B)** Schematic representation of the breeding strategy used in the present study to generate cell-specific IL-1R1 restored (A) and knockout (B) mouse lines, as well as their respective WT littermates. A shows the breeding strategy used to generate *Trpv1<sup>Cre::Il1r1<sup>tr</sup></sup>* mice, whereas B shows how *Trpv1<sup>Cre::Il1r1<sup>fl/fl</sup></sup>* mice were generated by taking advantage of the Cre-LoxP system. The *Trpv1<sup>Cre::Il1r1<sup>tr</sup></sup>* mouse line was used to restore IL-1R1 expression specifically and only in TRPV1<sup>+</sup> cells, while the *Trpv1<sup>Cre::Il1r1<sup>fl/fl</sup></sup>* line was used to knock out the *Il1r1* gene specifically in TRPV1-expressing cells. FL, floxed allele; he, heterozygous; ho, homozygous.

Table S1 is provided online as a separate Excel file and lists the differentially expressed genes associated with neuropeptides, neuromodulators, and neurotransmitters among the different DRG neuronal subtypes using scRNA-seq raw data.